Comparison of scour around two eccentric piers in clear water condition

A thesis submitted towards partial fulfilment of the requirements for the degree of

Master of Engineering

in

Water Resources and Hydraulic Engineering

Submitted by

HIMANGSHU ROY

Exam. Roll No. –M4WRE22019

Registration No. – 127320of 2014-15

Under the guidance of

Dr.SUBHASISH DAS

Associate Professor

School of Water Resources Engineering, Jadavpur University

&

Dr.RAJIB DAS

Assistant Professor

School of Water Resources Engineering, Jadavpur University

School of Water Resources Engineering

M.E. (Water Resources & Hydraulic Engineering)

Course affiliated to ***Faculty Council of Engineering & Technology***

Jadavpur University

Kolkata-700032, West Bengal, India

2022

Declaration of Originality and Compliance of Academic Ethics

I hereby declare that this thesis contains a literature survey and original research work by the undersigned candidate, as part of my **Master of Engineering** in **Water Resources and Hydraulic Engineering** in the Faculty Council ofInterdisciplinary Studies, Law & Management, Jadavpur University during the academic session 2021-22.

All information in this document have been obtained and presented in accordance with academic rules and ethical conduct.

I also declare that, as required by these rules and conduct, I have fully cited and referenced all material and results that are not original to this work.

Name	**:**	**Himangshu Roy**
Exam. Roll Number	**:**	**M4WRE22019**
Thesis Title	**:**	**Comparison of scour around two eccentric piers in clear water condition**
Signature with Date	**:**	

M.E. (Water Resources & Hydraulic Engg.)course affiliated to
Faculty Council of Engineering & Technology
Jadavpur University
Kolkata, India

Certificate of Recommendation

This is to certify that the thesis entitled "***Comparison of scour around two eccentric piers in clear water condition***" is a Bonafide work carried out by **Mr. Himangshu Roy** under our supervision and guidance for partial fulfilment of the requirement for the Post Graduate Degree of Master of Engineering in Water Resources and Hydraulic Engineering during the academic session 2021-22.

THESIS ADVISOR
Dr. Subhasish Das
Associate Professor
School of Water Resources Engineering
Jadavpur University

THESIS ADVISOR
Dr.Rajib Das
Assistant Professor
School of Water Resources Engineering
Jadavpur University

DIRECTOR
Prof. (Dr.) Pankaj Kumar Roy
School of Water Resources Engineering
Jadavpur University

DEAN
Prof. (Dr.) Subenoy Chakraborty
FacultyCouncil of Interdisciplinary
Studies, Law & Management
Jadavpur University

M.E. (Water Resources & Hydraulic Engg.)course affiliated to Faculty Council of Engineering & Technology Jadavpur University
Kolkata, India

CERTIFICATE OF APPROVAL **

This foregoing thesis is hereby approved as a credible study of an engineering subject carried out and presented in a manner satisfactorily to warranty its acceptance as a prerequisite to the degree for which it has been submitted. It is understood that by this approval the undersigned do not endorse or approve any statement made or opinion expressed or conclusion drawn therein but approve the thesis only for the purpose for which it has been submitted.

Committee of

Final Examination

for the evaluation

of the thesis

** Only in case the thesis is approved.

ACKNOWLEDGEMENTS

I express my sincere gratitude to my supervisors, ***Dr. Subhasish Das,*** *Associate Professorand* ***Dr. Rajib Das****, Assistant Professor, School of Water Resources Engineering, Jadavpur University, under whose supervision and guidance this work has been carried out. It would have been impossible to carry out this thesis work with confidence without their wholehearted involvement, advice, support and constant encouragement throughout. They have not only helped me in carrying out my thesis but also have given me valuable advice to proceed further in my life.*

Iwould also express my sincere gratitude to ***Prof. (Dr.) Asis Mazumdar****and****Prof. (Dr). Pankaj Kumar Roy*** *of School of Water Resources Engineering, Jadavpur Universityfor their valuable suggestions.*

I also express my sincere thanks to ***Mr. Buddhadev Nandi,*** *Research Scholar; of the School of Water Resources Engineering, Jadavpur University for his unconditional support and affection during my work. Also, thanks to my classmate* ***Mr. Piyush Prasad Gahlaut****for his help.*

Thanks, are also due to all staff of the School of Water Resources Engineering and the Regional -cum-Facilitation Centre (RCFC), NMPB, Jadavpur University for their help and support.

Date :

Place : Jadavpur University

Mr. Himangshu Roy
(Exam. Roll No:M4WRE22019)

ABSTRACT

Scouring is a natural phenomenon generated by the passage of water in a river or stream. It is most noticeable in alluvial materials, but the severely worn rock can also be vulnerable under specific conditions. Every year, numerous bridges fail, resulting in the loss of lives and property as well as some uncomfortable circumstances for transportation systems. Because of this, bridge designers are increasingly considering the flow-soil-structure interaction. The urban setting around the world is getting densely populated and facing heavy traffic with the increased number of vehicles. This opens the scope for the construction of new bridges beside already existing old ones.

On the other hand, in recent years tomaximize scour, several laboratory-based researches have been conducted using two or more in line, eccentric pier combinations keeping the aspect of the green dredging concept. The ultimate purpose is to shift the sediments to the bank of the channels without using any mechanical dredger.

Thus arises the need to study the interference of inline and eccentric piers. Therefore, a thorough investigation of scour depth around inline and eccentric piers in such conditions is highly desirable.

In this present study, the hydrodynamic consequences of different eccentric arrangements on scouring were investigated. Erosion and deposition patterns were studied around the front and eccentric piers at different time intervals along the flume. Inthis series of experiments, two identical circular piers are used to conduct twelve experiments. For the first six experiments,the inflow depth was kept constant at 12.7cm and for the remaining six experiments,the inflow depth was set fixed at 13.7cm. The eccentricity between the two piers was varied from 2-3.5 times the pier diameter. The longitudinal spacing between the upstream pier and the eccentric pier was also kept fixed. A fixed discharge of 27l/sand clear water condition was also maintained throughout the experiments. Six different eccentricities were used to run the experiments for 12 hours to observethe variation of scour with time. Several parameters like scour depth, width, length, area and volume were computed from the experimental outcomes. The results obtained from the series of experiments were carefully analysed to obtain the best arrangement for eccentricity which would be a beneficial aspect for bridge designers and dredging experts.

CONTENT

NOTATION

The following symbols are used in this dissertation work:

A = (hB) Cross-sectional area of flow [L^2];

a_{ps} = Planar area of scour [L^2];

a_{ss} = Surface area of scour [L^2];

a_s = Scour area [L^2];

b = Pier diameter [L];

B = Width of the tilting flume [L];

d_e = Eccentric pier scour depth [L];

d_{sf} =Scour depth at front pier [L]:

d_{se} = Scour depth at eccentric pier [L];

d_{16} = 16% finer sand diameter [L];

d_{50} = Median diameter of sand [L];

d_{84} = 84% finer sand diameter [L];

d_{90} = 90% finer sand diameter [L];

F_r = Froude number of flow [—];

g = Gravitational acceleration [LT^{-2}];

h = Approaching flow depth [L];

l_s = Scour length [L];

n = Manning's coefficient of roughness [—];

Q = Inlet discharge [L^3T^{-1}];

R_e = $\left(\frac{UH}{\nu}\right)$ Flow Reynolds number [—];

R_{*c} = $\left(\frac{u_{*c}R}{\nu}\right)$ Critical shear flow Reynolds number [—];

R_p = $\left(\frac{Ub}{\nu}\right)$ Pier Reynolds number [—];

e = ($3b$) Eccentricity [L];

S_0 = Bed slope [—];

U = Depth-averaged approaching flow velocity [LT^{-1}];

u_c = Critical velocity [LT^{-1}];

u_* = Shear velocity [LT^{-1}];

u_{*c} = Critical shear velocity [LT^{-1}];

V_s = Volume of scour [L^3];

w_s = Scour width [L];

ρ_f = Mass density of fluid [ML^{-3}];

ρ_s = Mass density of sand [ML^{-3}];

γ_f = Specific weight of fluid[$ML^{-2}T^{-2}$];

τ_o = Average bed shear stress [$ML^{-1}T^{-2}$];

τ_{oc} = Critical bed shear stress [$ML^{-1}T^{-2}$];

σ_g = Geometric standard deviation [—];

ν = Kinematic viscosity [L^2T^{-1}];

φ_r = Dynamic angle of repose [—];

Θ_c = Critical Shields parameter [—];

T = Time scale(T); and

t = Time (T).

Chapter 1

1.1Introduction

Scour is a natural phenomenon generated by rushing water's erosive impact on the bed and banks of alluvial rivers. Scour, in other terms, is the erosion of streambed silt around a barrier in a flow field. Cheremisinoff *et al.* (1987) defined scour as the lowering of the river bed due to water erosion, which has the potential to expose the foundations of structures such as bridges. Scour was characterized by Breusers *et al.* (1977) as a natural phenomenon created by the movement of water in rivers and streams. The scouring mechanism may endanger the structural integrity of hydraulic structures including bridges. When the foundation of the structures is compromised, this might lead to ultimate failure. A succession of bridge failures during floods caused by pier scour have highlighted the significance of developing better methods of protecting bridges from the ravages of scour. Bridge construction in alluvial channels causes the waterway at the bridge site to constrict. The waterway's shrinking could produce substantial scour at that location. According to Hoffmans and Verheij (1997), local scour around bridge piers and foundations caused by flood flows is the leading cause of bridge failure. Among those who have worked on pier scour are Raudkivi and Ettema (1983), Ahmed and Rajaratnam (1998), Chiew and Melville (1987), and Breusers *et al.* (1977). In their laboratory investigation on flow past cylindrical piers set on smooth, bumpy, and movable beds, Ahmed and Rajaratnam (1998) evaluated the flow around bridge piers. Jia *et al.* (2002) performed a numerical modelling study to simulate the time-dependent scour development around a cylindrical pier built on a loose substrate in an open channel Chiew and Lim (2001). Link and Zanke (2004) investigated the time-dependent development of scour-hole volume at a circular pier in uniform coarse sand and produced a mathematical link between the scour volume and the maximum scour depth for water depth to pier diameter ratios ranging from one to two. However, just as scour depth is crucial in scour research, so is the time taken to reach a specific scour depth because scour holes take time to form. As a result, it is vital to comprehend the evolution of the local scour hole over time.

Every year, numerous bridges fail, resulting in the loss of lives and property as well as some uncomfortable circumstances for transportation systems. The potential losses from bridge failures, as well as the necessity to protect against them, have encouraged a greater knowledge of the scour process, as well as improved scour prediction methods and equations. Under-prediction of pier scour depth can result in bridge failure, whereas over-prediction results in excessive resource spending in terms of building expenses. Because of this, bridge designers are increasingly considering the flow-soil-structure interaction. Achieving the safest design in light of local and regional characteristics is the most crucial factor to take into account at this stage. This is typically based on calculations of the maximum scour depth at bridge structural components and the geometrical features of the scour hole surrounding them.

The flow conditions, sediment characteristics, structure characteristics, and scouring duration are the main factors affecting the scour and deposition around the structure. As the number of structures in a river increases, the interaction between the structures will have a stronger impact on the surrounding bed profile. Local scour can be classified as "clear-water scour" or "live-bed scour." In clear

water scour, bed materials are removed from the scour hole but not replenished by the approach flow, whereas in live-bed scour, the scour hole is constantly supplied with sediment by the approach flow and an equilibrium is reached when the average amount of sediment transported into the scour hole by the approach flow equals the average amount of sediment removed from the scour hole over time. Under these conditions, the local scour depth changes around a mean value on a regular basis. The interplay of flow around a bridge pier and the erodible sediment substrate surrounding is quite complex.

In this study, the scour characteristics around two circular piers-placed eccentrically to each other were investigated.All the experiments were carried out in an experimental channel at the Fluvial Hydraulics Laboratory of the School of Water Resources Engineering, Jadavpur University. The study was confined to uniform cohesion less material and clear-water flow conditions.

1.2 Scouring around piers

Scouring is a natural phenomenon generated by the passage of water in a river or stream. It is most noticeable in alluvial materials, but the severely worn rock can also be vulnerable under specific conditions. It is caused by the erosive action of flowing water, which dissolves and erodes material from the stream bed and banks, as well as the vicinity of bridge piers and abutments. Scouring happens naturally as a result of river morphology changes and as a result of man-made structures. The following are the primary causes of scour:

(1) Depth of flow
(2) Pier width
(3) Velocity
(4) Froude number
(5) Bed materials

One of the primary reasons for bridge failure is scour. The scour destroys the bed materials around the bridge's foundation, exposing the foundation and jeopardizing the bridge's stability.

1.3 Classification of scour

Regardless of whether a structure is present, general scour happens in a river or stream as a result of natural processes. Man-made buildings or any other hazard may also induce scour in the river bed. Scour is divided into two types: (a) widespread scour and (b) localized scour. In addition, further sub-divisions of scour are depicted in **Fig 1.1**.

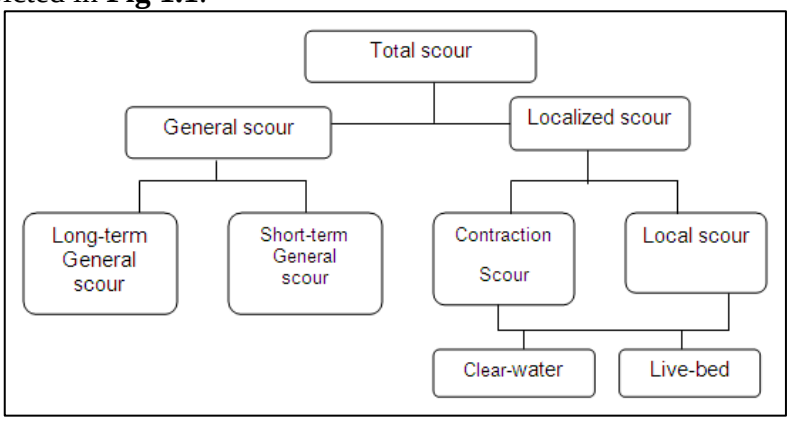

Fig 1.1 Types of scour

1.4 Local scour

Local scour is the erosion that takes place close to a pier, an abutment, an erosion control device, or another obstruction to the flow. These impediments speed up the flow and produce vortices that sweep the surrounding sediments away. Local scour depths are typically ten times greater than general or contraction scour depths in most cases. Local scour can cause failures by impairing the stability of riprap revetments and other structures. The following variables influence local scour:

1) Width of the obstruction.
2) Projection length of the obstruction into the flow.
3) Length of the obstruction.
4) Angle of the approach flow
5) Velocity of the approach flow
6) Size of the bed material.
7) Depth of flow.
8) Shape of the obstruction.
9) Bed configuration.

The depth of the scour is directly dependent on the width of the obstruction. Thus, the wider the obstruction, the deeper is the scour. Though not addressed by most empirical relations, the ratio of obstruction width to channel width is probably a better measure of scour potential than is the obstruction width alone. The projected length of obstruction into the stream affects the depth of scour. With an increase in the projected length of an abutment into the flow, there is an increase in scour.

Fig 1.2 Local scour around two eccentric piers.

The depth of the scour can increase with length, but only to a certain point. When the ratio of the projected length into the stream to the depth of the approaching flow is approximately 25, this limit is reached Larson, T. D. (1991). For straight sections, a structure's streamwise length has no discernible impact on the scour depth; however, when the structure is at an angle to the flow, the length has a significant impact. When a structure's length is doubled, the scour depth rises by as much as 33% at the same angle of attack. Some equations incorporate

the length factor by using the ratio of the structure's length to the flow's depth or width as well as the flow's angle of attack on the structure. Others incorporate flow in their equations using the projected area of the structure.

The scour depth can rise by a factor of 2 or more with an increase in flow depth. Depending on the shape of the abutment, the increase for bridge abutments ranges from 1.1 to 2.15. Along with the approach flow's velocity, scour depth also rises. Although the effect is typically a function of the time exposed to erosive flows, the size of the bed material affects scour depth. In other words, only the time it takes to reach the maximum or ultimate scour may be impacted by sediment size. Large particles in the bed material, like boulders or cobbles, may armour the scour hole's plate.

Local scour is greatly influenced by the shape of the structure as well as the flow's angle of attack on an obstruction. Structures that are angled to cause flow convergence tend to increase scour, whereas structures that are angled to cause flow divergence to tend to reduce scour. Streamlined structures effectively lower ultimate scour depths by weakening the horseshoe and wake vortices. The shape of the bed (bed configuration) in streams with sand beds influences the flow velocity and turbulence, which in turn influences the depth of scour. Both the local and global (contraction) scour can be accelerated by ice and debris. The extent of the growth is still largely unknown.

Chapter 2

2.1 Literature Review

Since the nineteen fifties, many researchers have performed experimental studies to understand the scour process at bridge piers and abutments as well as to derive scour depth predictors. Many studies have been conducted with the goal of predicting scour, and numerous equations have been developed by numerous researchers, including Laursen and Toch (1956); Liu et al. (1961);Shen *et al*. (1969); Breusers *et al*. (1977); Jain and Fischer (1979); Melville (1992); Abed and Gasser (1993); Richardson and Richardson (1994); Dey *et al*. (1995); Tseng *et al*. (1999); Graf and Istiarto (2002); Muzzammil and Gangadhariah (2003); Barbhuiya and Dey (2004); Marsh *et al.* (2004); Dey and Barbhuiya (2005); Dey and Raikar (2005); Lin *et al.* (2006); Ashtiani and Kordkandi (2012); Das *et al*. (2013); Khaple (2017) *et al.* Yilmaz (2017) *et al.* etc.

Melville (1975) [also see Melville and Raudkivi (1977)]was the pioneer to measure the turbulent flow field within a scour hole at a circular pier with the aid of the DISA Hot-Film Anemometer. The flow patterns were traced using the hydrogen-bubble method. He measured the flow field in the upstream axis of symmetry and the near-bed turbulence intensity for the case of a flat bed, intermediate, and equilibrium scour hole. He also estimated the bed-shear stresses from the measured near-bed velocities. A design method for the estimation of scour at cylindrical piers was presented by Melville *et al.* (1987). The method was based upon envelope curves drawn to experimental data derived mostly from laboratory experiments.

Melville and Sutherland (1988) presented a design method for the estimation of equilibrium depths of local scour at bridge piers. The method was based upon envelope curves drawn to experimental data derived mostly from laboratory experiments. The laboratory data included wide variations in flow velocity and depth, sediment size and gradation, and pier size, shape, and alignment. Local scour depth estimation was based upon the largest possible scour depth that can occur at a cylindrical pier, which was 2.4b, where b is the pier width. According to the method, this depth was reduced using multiplying factors where clear-water scour conditions exist, the flow depth was relatively shallow, and the sediment size was relatively coarse. In the case of nonrectangular piers, additional multiplying factors to account for pier shape and alignment were applied. The method of estimation of local scour depth was summarized in a flow chart.

Dargahi (1990) presented an extensive study containing the temporal evolution of the main flow features around circular bridge piers placed in a fixed sediment bed. He also visualized the flow field using air bubbles.Additionally, the bed shear stresses were measured with a Preston tube. Dargahi observed the simultaneous presence of various horseshoe vortices upstream of the leading pier front.

Breusers and Raudkivi (1991) found that reduction of scour depth due to a foundation located at an appropriate level below the initial bed level, should not be reposed on unless: Definite foretelling of bed level is possible, because the level of the river bed can go down extraordinarily during a flood in a particular

spread of the river, or the place of the pier may correspond with that of a moving stream channel in the cross-section. This exemplary note, which has been signified by others one of them was Melville (1988) has the main implying for design.

Kothyari *et al*. (1992a, b) discussed in a paper about scour depth. Since the scour depth was needed for the economical design of the pier foundation and determination of design scour depth was mainly based on the use of relationships for maximum scour depth in steady flow along with the design discharge. Time taken by the design discharge to scour to its full potential was generally larger than the time for which it runs. Hence, the computation of temporal variation of scour depth should form the basis of the design. Experiments were conducted on temporal variation of scour around circular bridge piers placed in uniform, non-uniform, and stratified beds under steady and unsteady clear-water flow. Considering the primary vortex in front of the pier to be the prime agent causing scour, a procedure was developed for computing the temporal variation of scour depth under these conditions. Since the maximum scour depth was the scour depth at the large time, the procedure was logically extended to obtain an expression for the same. Sediment nonuniformity and stratification were shown to have a significant effect on scour depth. The effect of these elements as well as that of unsteadiness of flow on scour depth are studied and taken into account in the proposed method of scour calculations.

Melville and Chiew (1999) considered the temporal development of clear-water local scour depth at cylindrical bridge piers in uniform sand beds in their studies. They infer that the scour depth after 10% of the time to equilibrium is between about 50% and 80% of the equilibrium scour depth, depending on the approach flow velocity.

Muzzammil and Gangadhariah (2003) investigated experimentally that the primary horseshoe vortex formed in front of a cylindrical pier which is the prime agent responsible for scour during the entire process of scouring. A simple and effective method was employed to obtain the time-averaged characteristics of the vortex in terms of parameters relating to variables of flow, pier and the channel bed. An expression for the maximum equilibrium scour depth was also developed from the vortex velocity distribution inside scour hole. The resulting scour prediction equation was found to give better results compared to the results of well-known predictor models when applied to model scour data.

Barbhuiya and Dey (2004) obtained similar results from a semicircular pier arrangement placed at the channel sidewall. The vortex size, vortex velocity and vortex strength were determined in terms of the relevant hydraulic and geometric parameters and the temporal scour hole evolution. These flow features govern the scour advance. In contrast to most other studies, a generalized approach was selected to determine the velocity distribution. The knowledge of these coherent plane flow structures allows estimating the acting bed-shear stresses, a topic dealt with in a forthcoming study.

Marsh *et al*. (2004) presented a comparison of four methods for predicting the incipient motion conditions of a uniform sand bed. The four methods are: (1) the Shields diagram, (2) an empirical approach, (3) a method derived from the resolution of rotational forces and (4) a simplified resolution of rotational forces with a variable lift force coefficient. The four methods were used to predict the incipient motion conditions for 97 experimental runs taken from seven independent experimental flume studies. The effectiveness of predicting depth-

averaged incipient motion velocity for each of the four methods was compared. The simplified resolution of the rotational forces model and Shields method were most successful in predicting the incipient motion velocity. The slope of the line of best fit for plots illustrating predicted versus measured incipient motion velocity was similar (slope=0.63, 0.65, respectively), illustrating that both methods provide a similarly justifiable prediction of depth-averaged incipient motion. The empirical method was the least successful at predicting the measured incipient motion conditions.

Dey and Barbhuiya (2005) stated a semi-empirical model that presented to compute the time variation of scour depth in an evolving scour hole at short abutments (abutment length/flow depth ≤1), namely the vertical wall, 45° wing wall, and semicircular, in uniform and non-uniform sediments under clear water scour condition based on the concept of the conservation of the mass of sediment, considering the primary vortex system as the main agent of scouring, and assuming a layer-by-layer scouring process. Experiments were conducted for time variation and equilibrium scour depths at different sizes of vertical walls, 45° wing walls and semicircular abutments in uniform and no uniform sediments under limiting clear water scour conditions.

Dey and Raikar (2005) derived an expression to estimateclear-water scour depth at circular and square piers, embedded in a sand bed overlain by a thin armour layer of gravels, which was experimentally studied. Depending on the pier width, flow depth, armour gravel, and bed-sand sizes, three cases of scour holes at piers in armoured beds were recognized. A comparison of the experimental data shows that the scour depth at a pier with an armour layer under limiting the stability of the surface particles was greater than that without an armour layer for the same bed sediments if the secondary armouring formed within the scour hole is scattered. The equations of maximum equilibrium scour depths at piers in armoured beds for these cases were proposed. On the other hand, the scour depth with an armour layer was less than that without an armour layer for the same bed sediments when the scour hole was shielded by the compact secondary armour layer.

Das *et al.* (2014) conducted an experimental study of the flow pattern and characteristics of a local equilibrium scour around a set of two identical shaped equilateral triangular piers (sides facing the approaching flow) placed in the longitudinal direction to the flow with an eccentricity (transverse distance). Das *et al.* (2015) also carried out an experimental study of the flow pattern and characteristics in a local equilibrium scour around a set of identical circular piers placed eccentrically. Here, the eccentricity and longitudinal spacing were equal to three times of pier width and 0.5 times the scour affected length in the equilibrium condition of a single pier. The maximum depth of the scour at the eccentric rear pier was about 44% greater than that in the single pier case. In addition, the maximum depth of the scour hole at the upstream of the inline front pier was about 29% more than that in the single pier case. Das *et al.* (2016) then determined the equilibrium scour geometry around two circular, square, and equilateral triangular piers, positioned in in-line front and eccentric rear arrangement, is determined by carrying out 19 clear water scour tests. Here the eccentricity was kept constant with the varying longitudinal spacing (l) from 0.25, 0.375, 0.5, 0.625, and 0.75 times the maximum equilibrium scour-affected

length for a single-pier test (L). At l = 0.75L, the maximum scour depth at the eccentric rear pier is found about 45–60% greater than that in the single-pier case. In addition, at l equal to 0.75L, the maximum depth of the scour hole at the upstream of the in-line front pier is about 35% more than that in the single-pier case. The reason may be the effect of reinforcing scour mechanism. The diversion angle of the scour and also the deposition were found more on the side of the eccentric pier.

Das and Mazumdar (2015) carried out an experimental study to investigate the horse-shoe vortex and flow characteristics in a local equilibrium scour hole around two identical cylindrical piers placed along the flow with an eccentricity and concluded that the eccentric arrangement of piers plays an important role in the formation of greater scour depth at the eccentric rear pier.

Das *et al.* (2015*b*) examined the local equilibrium scour features around a set of two identical circular, square, and triangular-shaped piers positioned in the flow's longitudinal direction with a constant eccentricity (transverse distance). The study's major goal was to investigate how the kind of scouring changed as a result of the mutual interference of one pie on another with various longitudinal distances of 0.25, 0.375, 0.5, 0.625, and 0.75 times the scour-affected lengths for a single pier experiment. The study of the results was primarily concerned with the change of specific non-dimensional equilibrium scour parameters with effective pier width.

Jaman *et al.* (2017*a*, *b*) conducted experiments ata clear water equilibrium scour condition to measure flow formations in local scour holes around three identical circular shaped piers arranged inline and eccentrically in staggering manners. Two inline piers were positioned toward flow, and an eccentric one was placed in the middle region of the two inline piers. The experiments were done for an approach flow depth of 0.125 m on the uniform bed of sand particles having a 0.825 mm median diameter. The hydrodynamic consequences of the three-pier arrangement on scour were investigated here. The contour profiles of scour were well addressed around the piers. The maximum equilibrium depth of all scour holes gauged for the inline front, eccentric-middle and inline-rear piers were about 40, 61 and 15% larger than the depth for one single-pier experiment. Also, these depths at inline-front, eccentric-middle and inline rear piers were more than two pier cases with the inline front eccentric rear arrangement. The dune formation was found more on the side of the eccentric pier (away from the line of symmetry). The diversion angle for sediment shifting was found to be more on the side of the eccentric pier.

Khaple *et al*. (2017) presented three kinds of pier arrangement - (i) two piers in tandem, (ii) two piers in a staggered arrangement, and (iii) three piers in symmetrically staggered arrangements. In the arrangement of two piers in tandem, the equilibrium scour depth at the downstream pier decreased with an increase in the downstream distance up to approximately eight times pier diameter and then increases with a further increase in downstream distance. However, the scour depth at the downstream pier was always smaller than that at the upstream pier. In the arrangement of two staggered piers, the scour depth at the downstream pier for e/b = 4, where e is the offset distance and b is the pier diameter, was the same as that of the upstream pier at S = 8b, where S is the stream-wise spacing or distance between piers. Further, for three piers in a

staggered arrangement, as the lateral spacing between downstream piers increased, the equilibrium scour depth at the downstream pier decreased.

Yilmaz *et al.* (2017) showed that for the efficient design of bridge pier footings, computation of time-evolution of scour depth around bridge piers is essential. They developed a semi-empirical model to estimate the temporal variation of clear-water scour depth at a couple of identical cylindrical uniform piers in tandem arrangement. The experiments were made using different pier sizes, pier spacings, and flow intensities. The model development was based on the sediment continuity approach and volumetric sediment transport rate from the scour hole using a sediment pickup function. The model results were presented as design charts giving the relation between dimensionless scour depth and time for practical use. Results, in the tested range of the proposed model, were in relatively good agreement with the experimental results.

Das *et al.* (2019) investigated the relative scour situation near three pier groupings. The scour geometries were shown when two tandem piers are placed in line with one another and a third pier is placed eccentrically in the middle of the tandem piers. Laboratory scale experiments were physically performed by gradually varying the intermediate longitudinal spacing between tandem piers. After each experimental run, the scour formation around the pier group and the dune formation downstream of the pier group are investigated.

Chapter 3

3.1 Local scour mechanism

The boundary layer flow past a cylindrical pier undergoes a three-dimensional separation. This separated shear layer rolls up along the obstruction to form a vortex system in front of the element which is swept downstream by the river flow. Viewed from the top, this vortex system has the characteristic shape of a horseshoe and is thus called a horseshoe vortex (**Fig 3.1)**, The formation of the horseshoe vortex and the associated down flow around the cylindrical pier results in increased shear stress and hence a local increase in sediment transport capacity of the flow. This leads to the development of a deep hole (scour hole) around the cylindrical pier, which in turn, changes the flow pattern causing a reduction in shear stress by the flow thus reducing its sediment transport capacity. The temporal variation of scour and the maximum depth of scour at bridge elements therefore mainly depend on the characteristics of flow, pier and river-bed material. The formation of the horseshoe vortex and the associated down flow cause scour at the cylindrical pier, abutment and spur dike.

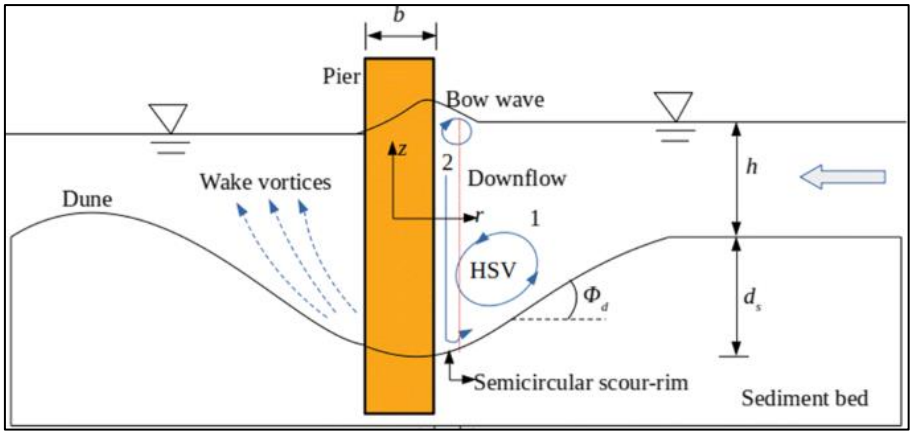

Fig 3.1 Scour mechanism at the cylindrical pier

The mechanism of scour around bridge piers was studied by Kothyari *et al.* (1992*a*, *b*) whereas studies on the mechanism of scour around abutments and spur dikes are available in Kothyari and Ranga Raju (2001).

3.2Horseshoe vortex and downflow

The flow deflected by sediment embedded bridge piers causes scour at its foundations. Scour may endanger the stability of the complete bridge structure. In bridge hydraulics, circular-shaped pier foundations are commonly used. Due to the similar flow structures of airflow around circular bodies in wind tunnels, the

basic researches concern flow visualization in aerodynamics. The main flow features involve a vertically deflected flow along the cylinder front, a horseshoe vortex system upstream of the cylinder, a flow separation beside the cylinder and a wake zone downstream of it shown in **Fig. 3.2,** For all flow conditions a horseshoe vortex system consisting of at least two vortices.

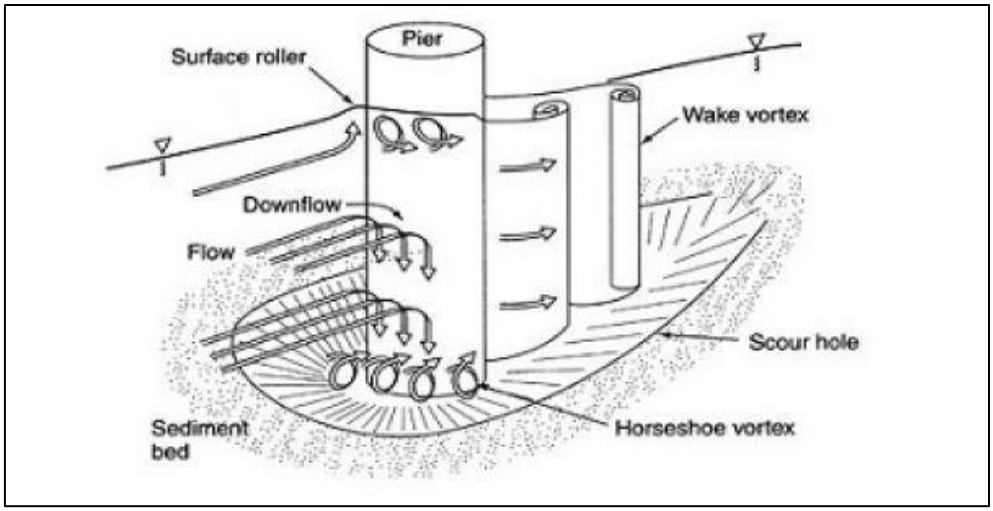

Fig 3.2 Mechanismof horseshoe vortex

The horseshoe vortex in front of the pier is the prime agent causing scour as said by Kothyari *et al.* (1992) assuming a layer-by-layer scouring process as said by Dey (1999). Tseng *et al.* (1999) said near the upstream face of the pier there exists a downflow which joins the separated flow to form the horseshoe vortex stretched around the pier.

3.3Wake vortex

Wake vortices form at the downstream side of piers and are the result of flow separation at the sides of the pier. Called cast-off vortices by Raudkivi (1986), these have vertical axes. One vortex develops on one side, sheds away, and is convicted downstream. Immediately, other forms on the other side, finally shedding also. The wake vortices dissipate as they move downstream. The frequency of vortex shedding is directly proportional to the approach velocity and inversely proportional to the pier diameter.

Information on wake vortex scour at bridge piers is particularly scanty. As wake vortex scour occurs at the downstream of the pier, it has little or no destructive potential. Because the horseshoe vortex scour occurs at the face of the pier and threatens to undermine the pier, this type of scour has been given considerable theoretical thought by Bruesers *et al.* (1977) and is well-documented with model studies by Raudkivi (1986).

Knowledge about wake vortex scour due to bridge piers has come mainly from a few laboratories'experiments Melville (1975). To describe the scouring action, Melville wrote "each of the concentrated vortices acts with its low-

pressure centre as a vacuum cleaner", picking up material from the bed, which is then transported downstream.

At most bridges, wake vortex scour is insignificant and confluence scour does not exist. In clear-water Rivers flowing on fine sand, these two forms of local scour can be very large. The deep scour holes downstream from the large circular piers (10 and 15 m in diameter) at the Tahrir and Imbaba Bridges over the Nile River in Cairo, Egypt was produced by the conflicting velocity fields at the intersection of the wake vortex streams from adjacent piers. The depths of scour due to these wake vortices are now 8 to 11 m where the normal depth of flow is approximately 8 m. Confluence scour where the main and side channel join upstream from the Imbaba Bridge was 9 m in 1981 and 1987 and was aligned with the bisector of the intersection angle of the two channels. These depths of scour can be considered nearly clear-water scour as the bridges are in the backwater of the Delta Barrages, the velocity is less than 1 m/s and sediment transport are very low. There is concern that the holes may enlarge or move upstream endangering the piers and the bridges. We have made observations in the vicinity of the scour holes and have come to the conclusion that, in each case, the scour was caused by two streams of wake vortices from adjacent piers intersecting downstream. The vortices that result from the two conflicting velocity fields create local scour. At one bridge, the scour is enhanced by the vortices that occur at the confluence of the main channel and its side channel. This is known as confluence scour.

3.4Classification of scour parameters

3.4.1 Flow intensity

Flow intensity is defined as the ratio of the shear velocity (u_*) to the critical shear velocity (u_{*c}) or the ratio of the approach mean velocity to the critical mean velocity [Melville and Chiew (1999)]. Under the clear-water condition, the local scour depth in uniformly-graded sediment increases almost linearly with velocity to a maximum at the threshold velocity [Melville and Coleman (2000)]. The maximum scour depth is reached when the ratio $u_*/u_{*c}= 1$ and the corresponding maximum scour depth is called the threshold peak. As the velocity exceeds the threshold velocity, the local scour depth in uniform sediment first decreases and then increases again to a second peak, but the threshold peak is not exceeded provided the sediment is uniform.

3.4.2 Flow depth

The influence of flow depth on the scour depth has been discussed by many authors [e.g., Breusers and Raudkivi (1991); Melville and Coleman (2000)]. The presence of the pier in the channel causes a surface roller around the pier and a horseshoe vortex at the base of the pier. Flow depth affects local scour depth when the horseshoe vortex is affected by the formation of the surface roller (or bow wave) that forms at the leading edge of the pier. The two rollers, (i.e., the bow wave and the horseshoe vortex) rotate in opposite directions. In principle, as

long as there is no interference between the two rollers, the local scour depth does not depend on the flow depth but depends only on the pier diameter.

In such an instance, often called deep flow, the local scour is said to occur at narrow piers. As the flow depth decreases, the surface roller becomes relatively more dominant and causes the horseshoe vortex to be less capable of entraining sediment. Therefore, for shallower flows, the local scour depth is reduced. Subsequently, in a very shallow flow, the local scour is dependent on the flow depth and the local scour is said to occur at a wide pier.

3.4.3 Pier width

Experiments have clearly shown that it is possible to relate the scour depth to the size of the pier (Breusers et al., 1977). This observation can be explained physically by the fact that scouring is due to the horseshoe vortex system whose dimension is a function of the diameter of the pier. It has also been observed that the horseshoe vortex, being one of the main scouring agents, is proportional to the pier Reynolds number (R_p), which in turn is a function of the pier diameter.

For the same value of mean approach flow velocity, therefore, the scour depth is proportional to the pier width. The influence of pier size on the local scour depth is of interest when data from the laboratory are interpreted for field use (Breusers and Raudkivi, 1991).

Under clear-water conditions, pier size influences the time taken to reach the ultimate scour depth but not its relative magnitudey_s/b, if the influence of relative depth,h/b, and relative grain size b/d_{50} on the local scour depth are excluded (Breusers and Raudkivi, 1991). They also concluded that the volume of the local scour hole formed around the upstream half of the perimeter of the pier is proportional to the cube of the pier diameter (or the projected width of the pier). The larger the pier the larger the scour hole volume and also the longer is the time taken for the development of the scour hole for a given shear stress ratio.

3.4.4 Pier Shape

Piers are constructed of various shapes. The most common shapes used are circular, rectangular, square, rectangular with chamfered end, oblong, Lenticular and Joukowski. The effect of pier shape has been reported by many researchers [e.g., Breusers (1977), Breusers and Raudkivi (1991), Melville and Coleman (2000)].

The blunter the pier, the deeper the local scour has been a general conclusion. The shape of the downstream end of the pier is concluded to be of little significance to the maximum scour depth. The pier shape is often accounted for by using a shape factor. Melville and Chiew (1999) discussed shape factors for uniform piers whichare piers having constant sections throughout their depth, was proposed. The local scour depths for a variety of different pier shapes all have the same projected width (140 mm). From his results, a circular pier produced the least scour while a rectangular pier having blunt ends produced the most scour.

For piers tapered on the upstream and downstream faces, the slope, in elevation, of the leading edge of the pier affects the local scour depth. Downward-tapered piers induce deeper scour than does a circular pier of the same width.

3.4.5 Sediment Size

The effects of the grain size and the density of the sediment material are often expressed as a function of the critical flow velocity for the initiation of sediment motion. Breusers and Raudkivi (1991) reported on the work of Raudkivi and Ettema (1977) in which the effect of sediment size on the local depth of scour at a bridge pier was studied. The experiments were conducted under clear-water conditions and using a pier of diameter 7 cm and a flume 1.5 m in width. It was observed that a sediment size of$d_{50} \leq 0.7$ mm leads to the formation of ripples, whereas a sediment size of$d_{50} \geq 0.7$ mm does not cause ripples. It was further stated that the results for grain sizes which lead to the formation of ripples ($d_{50} \leq$ 0.7 mm) were different from those for larger grain sizes for which ripples do not form ($d_{50} \geq 0.7$ mm).

According to Raudkivi and Ettema (1996), for non-ripple forming sediments ($d_{50} \geq 0.7$ mm), experiments can be run successfully with a flow condition,$u_* \sim 0.95 u_{*_c}$, without the upstream bed being disturbed by the approach flow, whereas with finer sands ($d_{50} < 0.7$ mm) a flatbed cannot be maintained for the same flow condition. Therefore, if the sediment is uniform sand with grain size$d_{50} < 0.7$ mm, a flatbed cannot be maintained near the threshold shear stress condition because ripples will develop, with a small amount of general sediment transport taking place so as to replenish some of the sand scoured at the pier. Thus, true clear-water scour conditions cannot be maintained for this case.

3.4.6 Flow Froude Number

The Froude number is a dimensionless number comparing inertia and gravitational forces. It may be used to quantify the resistance of an object moving through water and compare objects of different sizes. Named after William Froude, the Froude number is based on the speed/length ratio as defined by him.

$$F_r = \frac{U}{\sqrt{gh}} \tag{3.1}$$

where, U is a characteristic velocity and For rectangular cross-sections with uniform depth h, For $F_r < 1$ the flow is called a subcritical flow, further for $F_r > 1$ the flow is characterized as supercritical flow. When $F_r \approx 1$ the flow is denoted as critical flow.

3.5 Angle of repose

The angle of repose also referred to as the angle of friction, is an engineering property of granular materials. The angle of repose is the maximum angle of a stable slope determined by friction, cohesion and the shapes of the particles. When bulk granular materials are poured on a horizontal surface, a conical pile

will form. The internal angle between the surface of the pile and the horizontal surface is known as the angle of repose and is related to the density, surface area, and coefficient of friction of the material. Material with a low angle of repose forms flatter piles than material with a high angle of repose. In other words, the angle of repose is the angle a pile forms with the ground.

The angle of repose is the steepest anglethat the surface of a mass of loose particulatematter makes with the ground. The angle of repose is affected by the size, mass, angularity, and dampness of the particles and by the force of downward acceleration, but it is consistent for a given material. Knowing the angle of repose of material in various circumstances is vital for engineers and landscapers, for example.

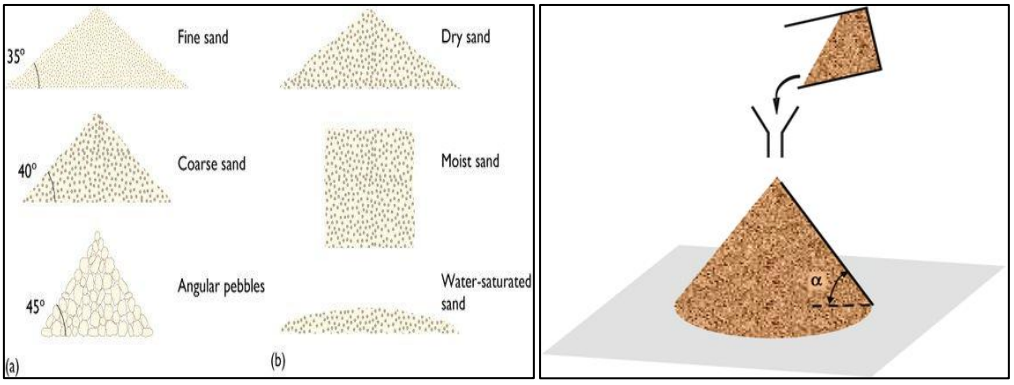

Fig. 3.5 Angle of repose

The way in which most people are familiar with the angle of repose is sand castles. Dry sand generally has an angle of repose of about 30°, so piled dry sand forms shallow inverted cones. When sand is dampened, the surface tension of the water binds the grains together, and the angle of repose is increased to more than vertical so that walls and towers and sea caves can be made. When sand is too wet, however, the water lubricates the grains instead of sticking them together, and the angle of repose is decreased to nearly zero. This should be required knowledge for anyone who is thinking of buying a house built on a sandbar.

Chapter 4

4.1 Objectives

The main goal of this study is to conduct experiments to demonstrate how the scouring varies around two eccentrically positioned circular piers. In the current study, attempts have been made to observe the nature of the scour depth that is developing around circular piers with respect to time. By adjusting the eccentricity between the piers, 12 experiments have been run with a fixed pier diameter of 0.07 m and inflow depth of 12.7 cm for the first six experiments and13.7cm for the next six experiments. The results of the experiments have been carefully analyzed to obtain the pier arrangement in which the maximum scouring is taking place by calculating the scour volume in each case. The experimental procedure followed is as under:

Table 4.1 Series of experiments conducted using circular piers

Experiment no.	Discharge (Q) (Lps)	Flow depth (h) (cm)	Pier diameter (b) (cm)	Spacing between piers		Froude No	U/u_c (%)
				Longitudinal	Eccentric		
1	27	12.7	7	5.185b	2b	0.24	79
2	27	12.7	7	5.185b	2.25b	0.24	79
3	27	12.7	7	5.185b	2.5b	0.24	79
4	27	12.7	7	5.185b	2.75b	0.24	79
5	27	12.7	7	5.185b	3b	0.24	79
6	27	12.7	7	5.185b	3.5b	0.24	79
7	27	13.7	7	5.185b	2b	0.21	72
8	27	13.7	7	5.185b	2.25b	0.21	72
9	27	13.7	7	5.185b	2.5b	0.21	72
10	27	13.7	7	5.185b	2.75b	0.21	72
11	27	13.7	7	5.185b	3b	0.21	72
12	27	13.7	7	5.185b	3.5b	0.21	72

4.2 Methodology

1) The flow depth in the flume was adjusted by a tailgate. The approaching flow depth (h) was maintained as 0.127 m for the first series of experimental runs and for the second series of experiments the approaching flow depth was maintained as 0.137m. The bed slopeS_0 (=1:2400)was kept constant throughout all the experiments.

2) The critical condition of the bed was examined before the experiment run using steps 2 to 6. The depth-averaged approaching flow velocity (U)was estimated using Manning's equation$\left(U = \frac{1}{n} R^{\frac{2}{3}} S^{\frac{1}{2}}\right)$. Here, the coefficient of roughness (n) was determined by using Strickler's formula$\left(n = \frac{1}{24} d_{50}^{\frac{1}{6}}\right)$. From the sieve analysis experiment, the median diameter of sand (d_{50})was determined as 0.784 cm from **Fig 4.1.**

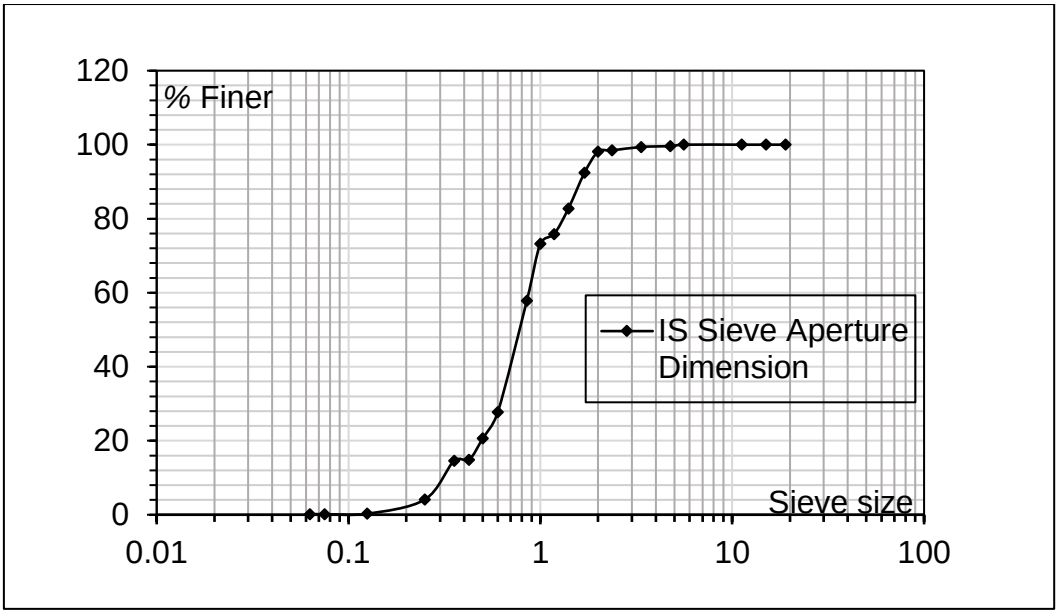

Fig 4.1 Grading curve

3) The critical bed shear stress (τ_{0c}) was determined by using the expression for the critical Shields parameter, $\Theta_c\left(=\frac{\tau_{0c}}{\Delta\rho_f g d}\right)$ which was developed by van Rijn (1984). From van Rijn's (1984) empirical equations of the Shields curve, the value of the critical Shields parameter was calculated where the particle parameter, $D_*\left(=d\left(\frac{\Delta g}{\nu^2}\right)^{\frac{1}{3}}\right)$= 21.218. Then the equation of critical bed shear stress becomes as $\tau_{0c}=0.0315\Delta\rho_f g d$(=0. 0.3969 N/m^2).

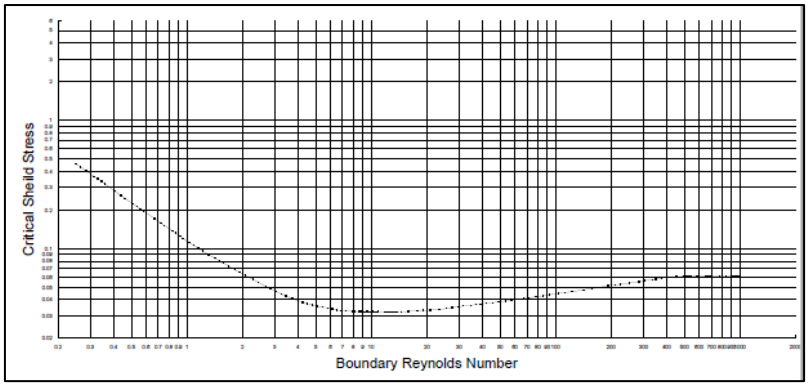

Fig 4.2 Shields diagram

5) Then critical shear velocity (u_{*c}) was calculated using $u_{*c}=\sqrt{\frac{\tau_0}{\rho_f}}$= 0.0196. Therefore u_c can be calculated from $\frac{u_c}{u_{*c}}=5.75\,log\left(\frac{h}{2d_{50}}\right)+6$where$u_{*c}, h$, d_{50} are already known. Now, u_c = 0.332 m/s for h =12.7 cm and u_c = 0.336 m/sfor h =13.7 cm.

6) Critical shear flow Reynolds number $R_{*c}\left(=\frac{u_{*c}R}{\nu}\right)$was determined at the 20^{0}C temperature of the water where R is the hydraulic radius.**Figure**

4.2,shows Shields' experimental results which relate critical Shields parameter (Θ) and (R_{*c}) is known as the Shields diagram(1936). The threshold of sediment motion occurs when $\Theta > \Theta_c$ or $\tau_0 > \tau_{0c}$ or $u_* > u_{*c}$.It is clear that the discharge during each experiment run was lower than the minimum discharge required for the incipient motion or threshold conditions of the bed particles. Therefore, it can be said that all the experiments were carried out under clear water scour conditions.

7) The depth-averaged approaching flow velocity (*U)* was set as about 79 % for h =12.7 cm. and depth average approaching flow velocity (U) was also set 72% for h = 13.7 cm and the critical velocity (u_c) of the uniform sand bed considering side-wall effect to satisfy the clear water condition i.e. the present research considered only clear water approach flow conditions described by a threshold/critical Froude number of $F_t = U/u_c = 0.79$ for h =12.7 cm and 0.72 for h = 13.7 cm (Dey and Raikar, 2007;Oliveto and Hager, 2002).The depth-averaged approaching flow velocity was determined from the measured vertical profile of the approaching flow velocity at 2 m upstream of the pier where the presence of the pier did not affect the approaching flow. Also, to satisfy clear water scour conditions, average bed shear stress (τ_0) must be less than or equal to critical bed shear stress (τ_{0c}). It was determined using the method proposed by Dey (2003).

8) Das *et al.* (2015) conducted experimental studies on local equilibrium scour around a set of two identical piers of different shapes placed at a constant eccentricity ($e = 3b$) to analyze the nature of scour evolved due to the effect of mutual interference of one pier on another, varying the longitudinal spacing between them. It was observed that maximum scour development was taken place at a longitudinal spacing of 5.185b. Therefore, based on this concept, the current study was conducted to analyze the effect of eccentricity along with the constant longitudinal distance of 5.185b to find the maximum and minimum scour by varying the eccentricity.

Chapter 5

5.1 Experimental setup

The experimental arrangement, data acquisition system and variables measured in the model study are described. A typical investigation of scour depth development around two eccentric piers has been carried out through various experiments. The experimental setup and conditions of the work are described in detail. All the experiments were conducted in the Fluvial Hydraulics Laboratory (**Fig. 5.1**) of the School of Water Resources Engineering at Jadavpur University, Kolkata.

Fig 5.1 Tilting flume used during the experimentation

5.1.1 Tilting Flume

The experiments are carried out in a recirculating flume 11 m long, 0.81 m wide, and 0.60 m deep (**Figs. 5.1-5.2**). The working section of the flume is filled with sand to a uniform thickness of 0.20 m. The length of the sand bed is 7m and the width is 0.81 m. The sand bed is located 2.9 m upstream from the flume inlet. The working section of the flume is made up of a steel bottom and Plexiglas side walls along two sides for most of its length to facilitate visual observations. The recirculating flow system is served by a centrifugal pump located at the upstream end of the flume.

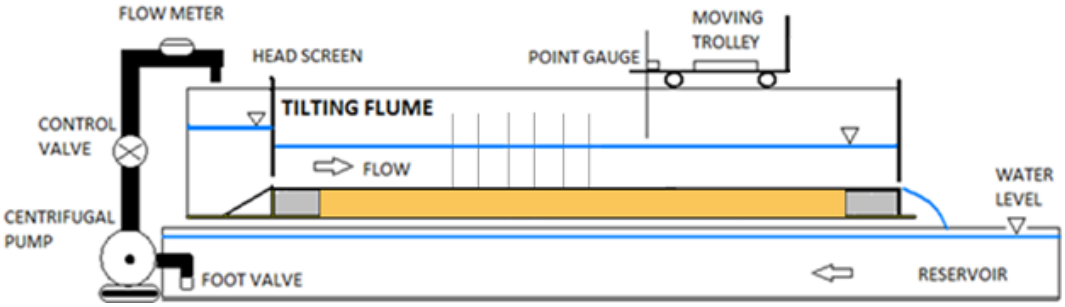

Fig 5.2 Schematic diagram of tilting flume

5.1.2 Pump

The hydraulic machines which convert the mechanical energy into hydraulic energy are called pumps. Hydraulic energy is in the form of pressure energy. The recirculating flow system is served with a 10hp, variable speed, centrifugal pump located at the upstream end of the flume (**Fig. 5.3**). Water flows through a 200 mm diameter pipe line which runs directly into the flume. The rpm of the pump is 1430; power is 7.5 kW, and maximum discharge is 30 l/s. There are two pumps for alternative use. To measure the discharge, water flows through a flow meter.

Fig 5.3 Pump used to recirculate the flow

5.1.3 Pier

In the present study, all two piers models were constructed using Perspex sheets. Two circular bridge piers models of diameter 7 cm have been used in the present study (**Fig. 5.4**). The height of the piers is 45.6 cm. During the experiment, it is kept in mind that the width of the experimental flume is more than eight times the pier diameter to avoid the wall friction factor.

Fig 5.4 Piers placed at the working section of the flume

5.1.4 Sand Bed

The shields diagram remains the most effective way of determining threshold conditions for uniform sediments. For given fluid density and viscosity and sediment density, the shields diagram can be used to obtain a plot of shear velocityu_{*c} against grain sized_{50}. The determination of threshold conditions for non-uniform sediment is not so clear-cut. The effects of particle size distribution may be important and thusu_c would depend on both the median grain sized_{50} and the geometric standard deviation, $\sigma_g=(d_{84}/d_{16})^{0.5}$ with non-uniform sediments, a flow can disturb the grain, removing some but simply rearranging others into a stable pattern that develops into an armoured bed and stabilizes. Such flow is considered here in to be above the threshold. Values ofu_c are found using a suggestion first made by Weill that many of the intermediate sizes will move when flow conditions based ond_{50} exceed the shields criterion.

A series of experiments are carried out on the sand bed material (**Fig. 5.5**). In the laboratory we measured the vibrating sieve analysis and specific gravity Sand particle sizes $d_{50}$is 0.784 mm,d_{16} is 0.43 mm,d_{84} is 1.438 mm andd_{90} is 1.62 mm. The geometric standard deviation of sediment size (σ_g)is 1.8. The density of the sand is 2.63. We have measured the sand particle size from the graph. Here we plot the grain size distribution and percent finer.

Small triangular sand waves with a long gradual upstream slope (approximately 6°) and short steep downstream slope (approximately 32°) are called ripples. In the case of fine sediments (d_{50}< 0.7 mm), ripples are formed, while coarse sediments usually form dunes. The wave lengths of ripples are usually shorter than 300 mm or approximately equaling 150d_{50}. It is assumed that ripples are formed if the viscous sub-layer is present when the threshold shear stress is just suppressed, while dunes are formed if the bed is hydraulically rough. The length of the ripples depends on the sediment size and the flow velocity but is essentially independent of the flow depth. Ripples may be superposed upon the upstream side of dunes.

Dunes are the bed –forms larger than ripples, whose profile is out of phase with the free surface profile. The stream-wise profile of a dune is roughly triangular with a mild upstream slope and a downstream slope approximately equal to the angle of repose. Dunes are formed in coarse sediment (d_{50}> 0.6 mm).

Above this, a zone of high turbulence exists, where a large production (and dissipation) of turbulent energy takes place. Near the zone of reattachment, the sediment particles are transported by the turbulence, even when the local bed shear stress is below its threshold value. On the upstream side of the dune, the bed shear stress drives sediment particles uphill until they pass over the crest and eventually are buried in the bed for a period. As sediment is transported from the upstream side and deposited on the lee side of a dune, the result is a slow continuous downstream migration of the dunes.

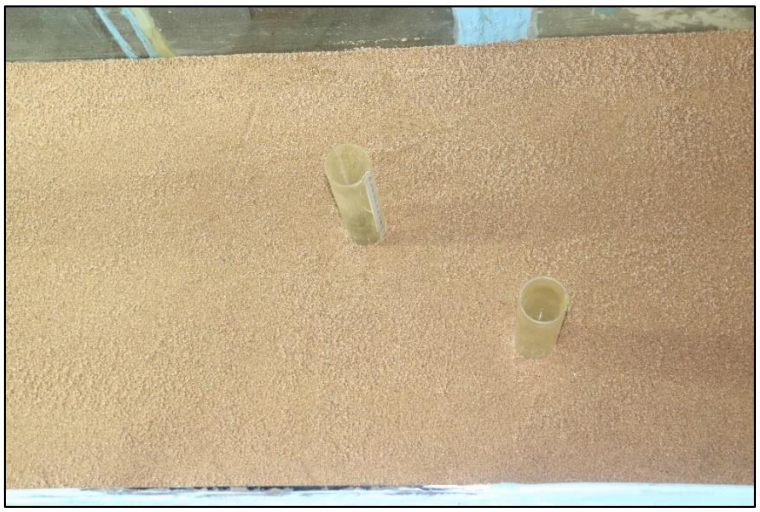

Fig 5.5 Experimental sand bed

After placing the piers in proper position with proper alignment properly flat sand bed was prepared. A very good experiment requires a properly prepared flat sand bed which is very essential for attaining good experimental results. A 3 m long and 0.81 m wide flat sand bed was prepared and the flatness of the sand bed was checked with a spirit level. The sand bed preparation was done for every new setup of piers arrangement.

5.2 Experimental procedure

The average bed shear stress was 0.39Pa and the angle of repose of bed sand and critical bed shear stress were estimated 34°and 0.40 Pa respectively. The flow depth in the flume was adjusted by operating a tailgate.The depth-averaged approaching flow velocity was found from the measured vertical profile of the approaching flow velocity at 2 m upstream of the pier where the presence of the pier did not affect the approaching flow.

Froude number (F_r)are 0.24 and 0.21, flow Reynolds number (R_e) and pierReynolds number (R_p) for all the experiments were calculated as 2.4×10^4, 2.25×10^4, 1.8×10^4, 1.8×10^4respectively.

The pier is first installed in the flume at the desired location. Before each experiment, care is taken to level the sand bed throughout the entire length of the flume and perpendicular to the pier structure. First of all, we have to produce a sand bed having a smooth, uniform surface, so we used a spirit level to check the uniformity of the bed surface. The uneven bed surface is levelled using a hand trowel. After that, we have to measure the bed level by point gauge randomly and check the levelling of the flume. The sand bed preparation is very key as for as the experiment is concerned. Unevenness or defect in the channel bed can cause damage to the experiment. Piers are constructed eccentrically with different conditions with the help of the single pier total scour length.

During the experiment, it was kept in mind that the width of the experimental flume is more than seven times the pier width to avoid the wall friction factor. The minimum value of the ratio between flume width and pier width is 6.25, as proposed by Raudkivi and Ettema (1983) which could be used without a measurable effect from the side walls on the local scour at the pier.

To start the experiment, the flume is slowly filled with water to the required depth from downstream. It should be noted that extra care is required when filling the flume with water, especially for an experiment of this nature where no sediment movement is allowed. Any deformity in the bed surface may develop ripples or dunes and general movement of the sand if the shear stress on the smooth bed is close to the critical shear stress. The pump is then turned on and the desired flow rate has been achieved by controlling the control valve and a bypass valve.

Concurrent with getting the pump up to speed, the tailgate is adjusted so as to maintain the correct depth of 0.127m for the first six experiments and 0.137 m for the next six experiments of flow in the flume. Throughout the experiment period, the location and magnitude of the point of maximum scour depth are around the upstream of the pier. The frequency of the scour depth varied throughout the experiment period. The rate of scouring is maximum in the period of 1 to 4 hoursand then less frequently thereafter. Here we have used the fibre transferring pier model. The run duration for all the experiments is 12 hours. After that, the pump is stopped to allow the flume to slowly drain without disturbing the scour topography.

Chapter 6

6.1 Results and discussion

A study of local erosion around two eccentric circular piers in clear-water conditions was carried out.After conducting all the six experiments for scour holes geometrical parameters like maximum scour depth, length of sediment shifted to the downstream, max-width of scouring deposition, hole surface area and the total volume of scouring deposited and scour volume were analyzed. Here total experiments were run for a total duration of 12 hours. The scour depth was measured with a help of a laser distance meter and the data obtained was analyzed with the help of surfer software to generate contour maps.

In this present study, the hydrodynamic consequences of different eccentric arrangements on scouring were investigated.Erosion and deposition patterns were studied around the front and eccentric piers at different time intervals along the flume.A total of 12 experiments were carried out with the same experimental conditions such as discharge, velocity, water depth, and bed material. The width of each pier was taken equal to 7 cm.

Each experiment was started with a flattened bed. While the outletvalve was closed, the flume was filled with water very slowlywithout disturbing the bed material, until the desired flow depthwas reached. Then the inflow valve was adjusted to the desireddischarge in the flume and the outlet valve was partially opened. The experiments were carried out for constant discharge of 27 l/s and constant flowdepth maintained at 12.7cm forthe first six experiments and 13.7cm for the next six experimentsfor each discharge. The experimental run duration for each experiment was 12 hours. Knowing that scour depth evolves rapidly at the beginning of theexperiments and gets slower towards the end, the scour depthmeasurements are recorded more frequently at thebeginning.In each experiment, the time series were frequent at the beginning such as 2,4,6,8,10,14,18,22,26, and 30 min.

In order to plot the contour profile, the water in the flume was drained after the completion of experiments and the sediment deposition was investigated by taking the depth at the scoured region with the help ofa laser distance meter.This procedure is repeated for theaforementioned experiment durations and experiments. The experimental outcomes are discussed below.

Table 6.1: The parameters kept constant throughout the series of experiments

Parameter	Values
Discharge (Q)	27 l/s
Longitudinal distance (l_o)	5.19b
Pier width (b)	7cm
Experimental duration (t)	12 hours

6.1.1 Experiment No. 1

This experiment was conducted for an eccentricity of 2b for 12 hours. Here, Fig 1a, Fig 1b, Fig 1c and Fig 1d denote the level bed before starting the experiment,duringexperiment flow condition, scour bed after drying the bed and the contour diagram respectively.

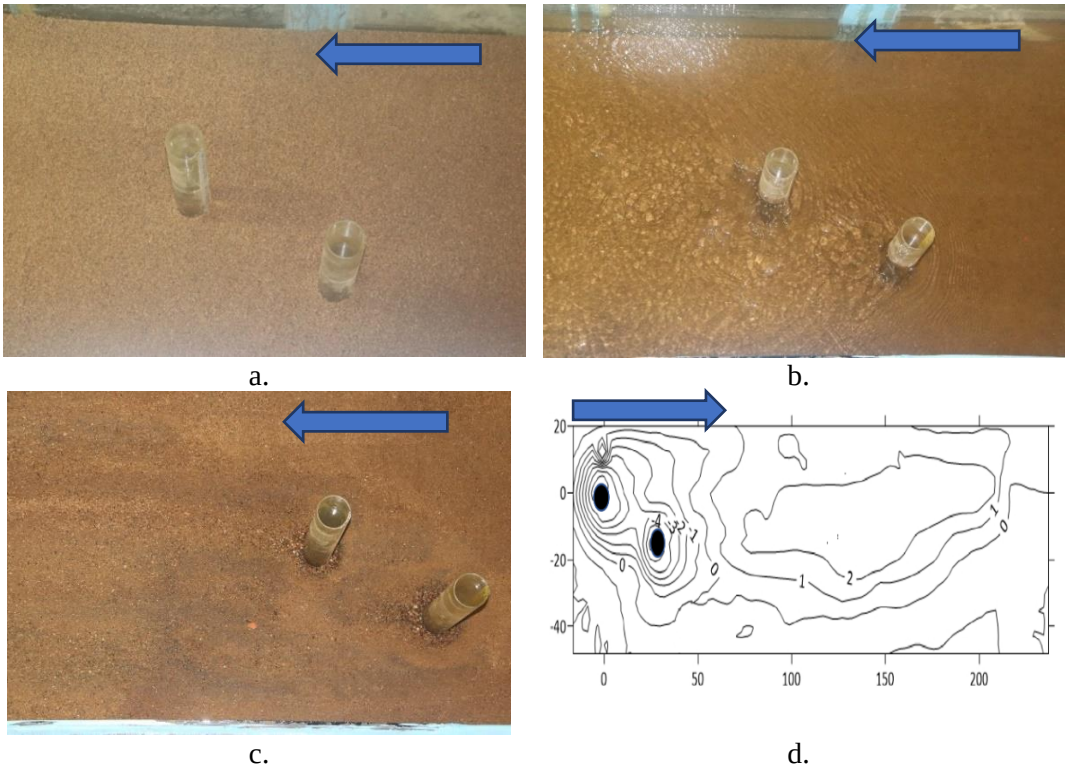

Fig 6.1.1 Experimental condition for experiment 1, *e* = 2 *b*,a. Level bed, b. During Experiment, c. Scour bed, d. Contour Map.

The values of subsequent scour depths were recorded with a help of the laser distance meter. The frequency of recording the scour depths was incremented with the passing of each hour. It was observed that the scour depth for both the piers, in this case, was maximum among the series of experiments conducted. The scour depth observed at the front pier was 0.069 m and that at the eccentric pier was 0.079m, after the completion of the experiment. The contour map was generated using surfer software. All the relevant results are given in Table 3.

6.1.2 Experiment No. 2

This experiment was conducted for an eccentricity of 2.25*b* for 12 hours. The values of subsequent scour depths were recorded with a help of the laser distance meter.

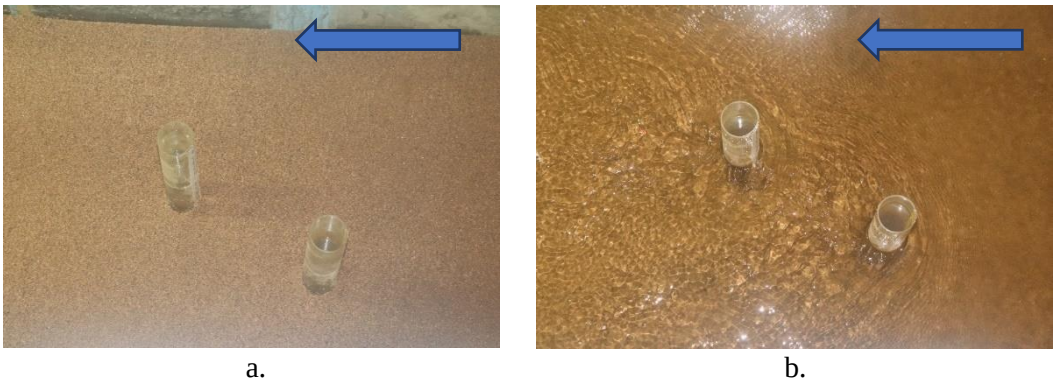

c.

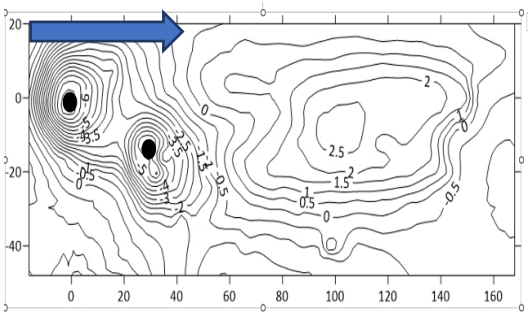

d.

Fig 6.1.2 Experimental condition for experiment 2, *e* = 2.25 *b*,a. Level bed, b. During Experiment, c. Scour bed, d. Contour Map.

The frequency of recording the scour depths was incremented with the passing of each hour. The scour depth observed at the front pier was 0.113 m and that at the eccentric pier was 0.121 m, after the completion of the experiment surfer software was used to generate contour maps.

6.1.3 Experiment No. 3

This experiment was conducted for an eccentricity of 2.5*b* for 12 hours. The values of subsequent scour depths were recorded with a help of the laser distance meter.

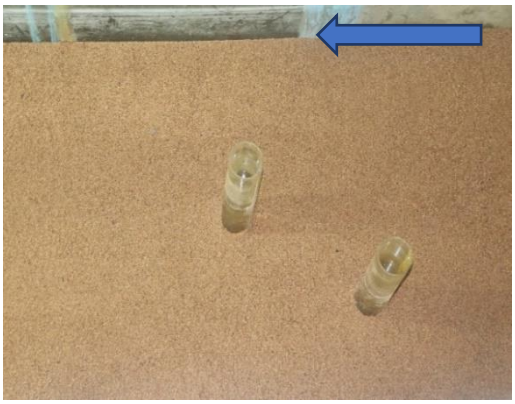

a.

b.

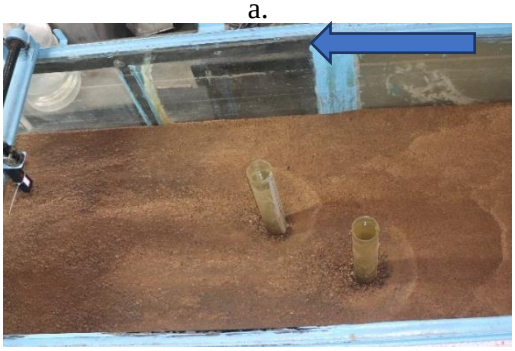

c.

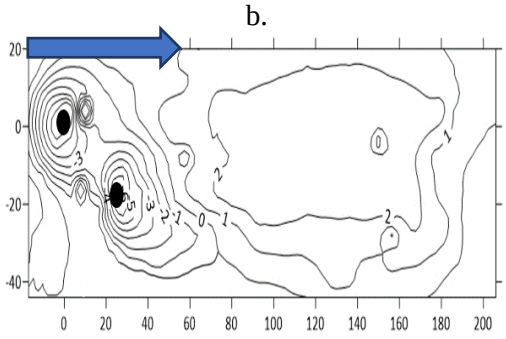

d.

Fig 6.1.3 Experimental condition for experiment 3, *e* = 2.25*b*b a. Level bed, b. During Experiment, c. Scour bed, d. Contour Map.

The frequency of recording the scour depths was incremented with the passing of each hour. It was observed that the maximum scour depth in this experiment was very close to the previous experiment i.e.,*e*= 2.25 *b*. The scour depth observed at the front pier was 0.126 m and that at the eccentric pier was 0.136 m, after the completion of the experiment.

6.1.4 Experiment No. 4

This experiment was conducted for an eccentricity of 2.75*b* for 12 hours. The values of subsequent scour depths were recorded with a help of the laser distance meter

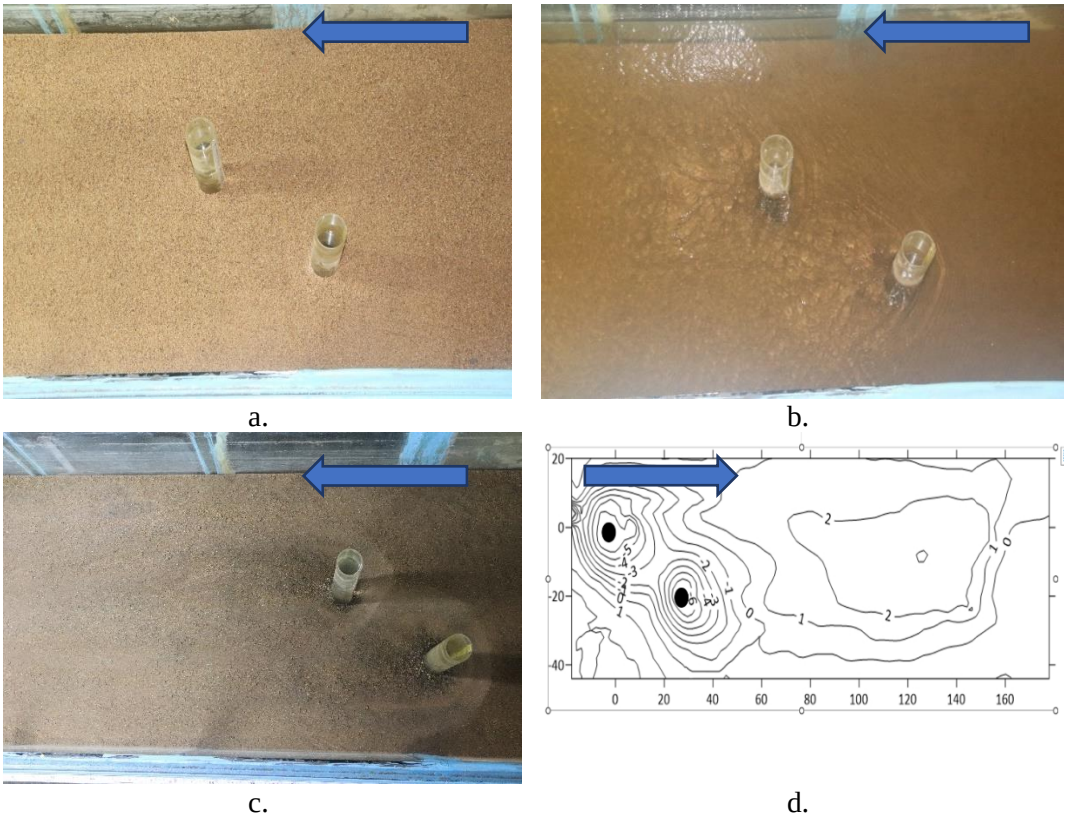

Fig 6.1.4 Experimental condition for experiment 4, *e* = 2.75*b*b a. Level bed, b. During Experiment, c. Scour bed, d. Contour Map.

The frequency of recording the scour depths was incremented with the passing of each hour. The scour depth observed at the front pier was 0.122 m and that at the eccentric pier was 0.139 m, after the completion of the experiment.

6.1.5 Experiment No. 5

This experiment was conducted for an eccentricity of 3*b* for 12 hours. The values of subsequent scour depths were recorded with a help of the laser distance meter. The frequency of recording the scour depths was incremented with the passing of each hour.

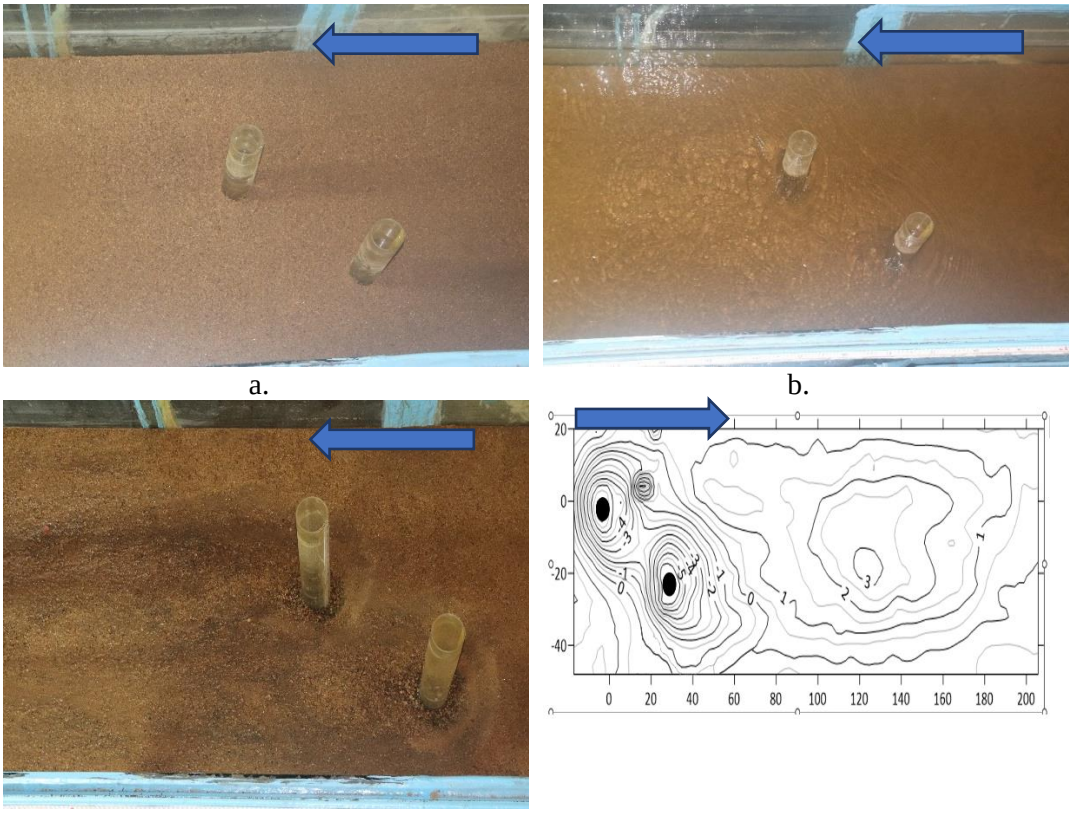

Fig 6.1.5 Experimental condition for experiment 5, $e = 3b$,a. Level bed, b. During Experiment, c. Scour bed, d. Contour Map.

The maximum scour depth observed at the front pier was 0.086 m and that at the eccentric pier was 0.106 m, after the completion of the experiment.

6.1.6 Experiment No. 6

This experiment was conducted for an eccentricity of 3.5*b* for 12 hours. The values of subsequent scour depths were recorded with a help of the laser distance meter.

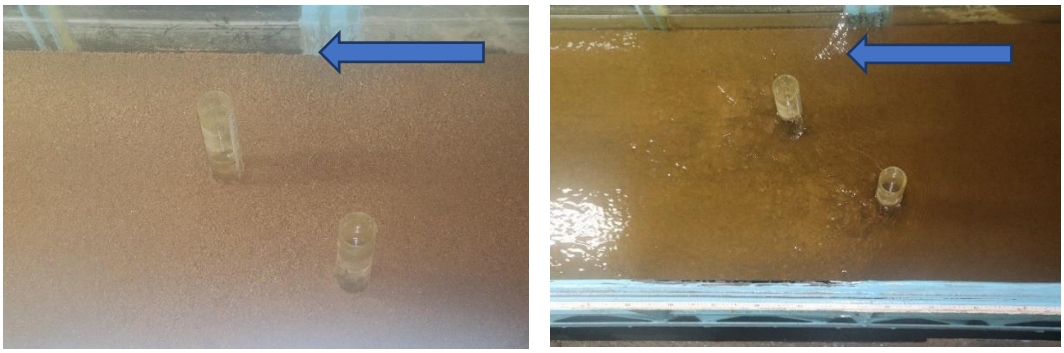

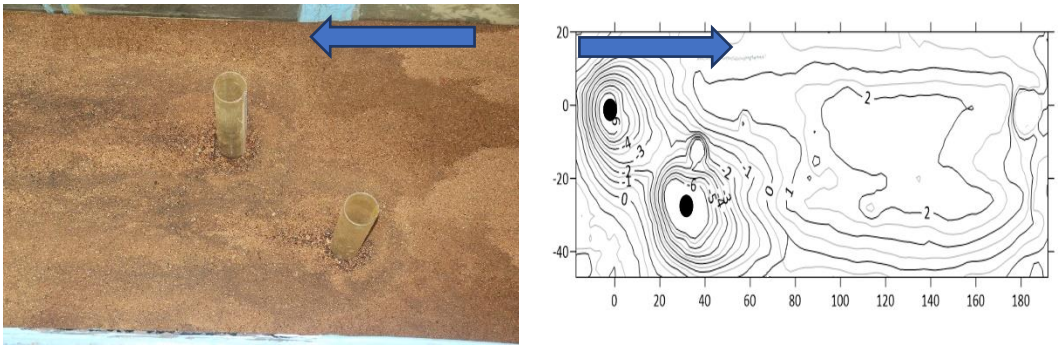

c. d.

Fig 6.1.6 Experimental condition for experiment 6, $e = 3.5b$,a. Level bed, b. During Experiment, c. Scour bed, d. Contour Map.

The frequency of recording the scour depths was incremented with the passing of each hour. The maximum scour depth observed at the front pier was 0.082 m and that at the eccentric pier was 0.093 m, after the completion of the experiment.

6.1.7Experiment No. 7

This experiment was conducted for an eccentricity of 2*b* for 12 hours. Here, Fig 1a, Fig 1b, Fig 1c and Fig 1d denote the level bed before starting the experiment, during experiment flow condition, scour bed after drying the bed and the contour diagram respectively.

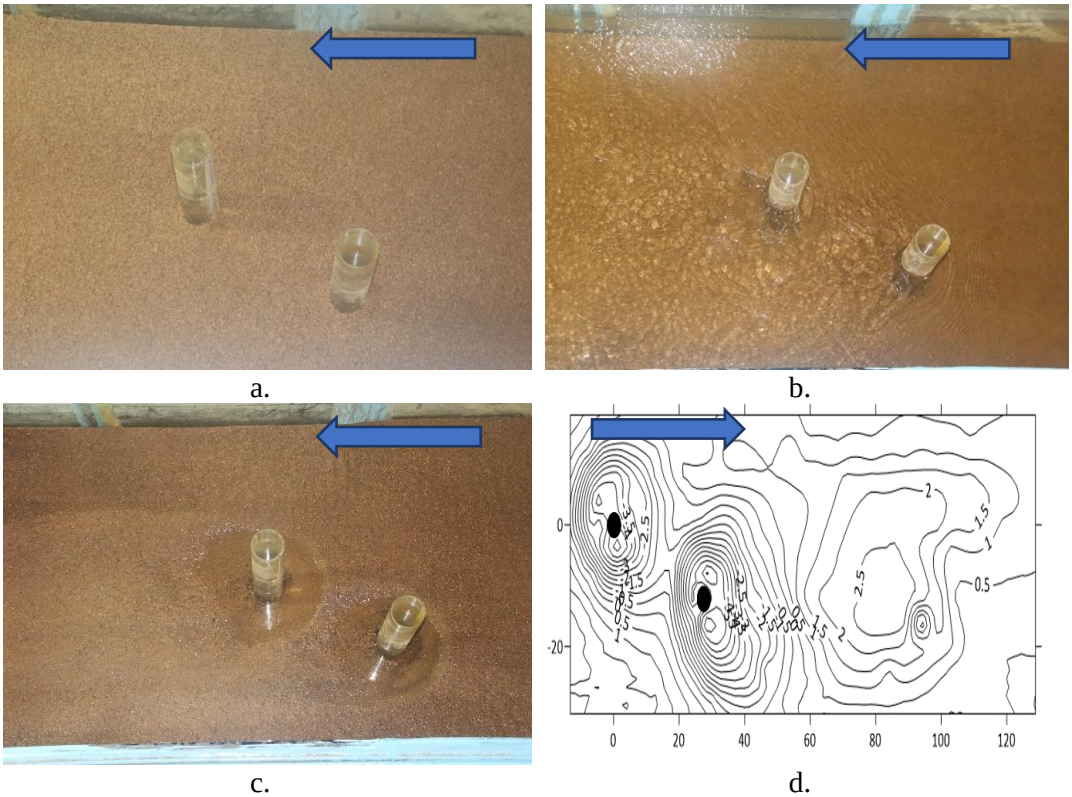

a. b.

c. d.

Fig 6.1.7 Experimental condition for experiment 7, $e = 2b$,a. Level bed, b. During Experiment, c. Scour bed, d. Contour Map.

The values of subsequent scour depths were recorded with a help of the laser distance meter. The frequency of recording the scour depths was incremented with the passing of each hour. It was observed that the scour depth for both the piers, in this case, was maximum among the series of experiments conducted. The scour depth observed at the front pier was 0.0701 m and that at the eccentric pier was 0.1015m, after the completion of the experiment. The contour map was generated using surfer software. All the relevant results are given in Table 3.

6.1.8Experiment No. 8

This experiment was conducted for an eccentricity of 2.25*b* for 12 hours. The values of subsequent scour depths were recorded with a help of the laser distance meter. The frequency of recording the scour depths was incremented with the passing of each hour.

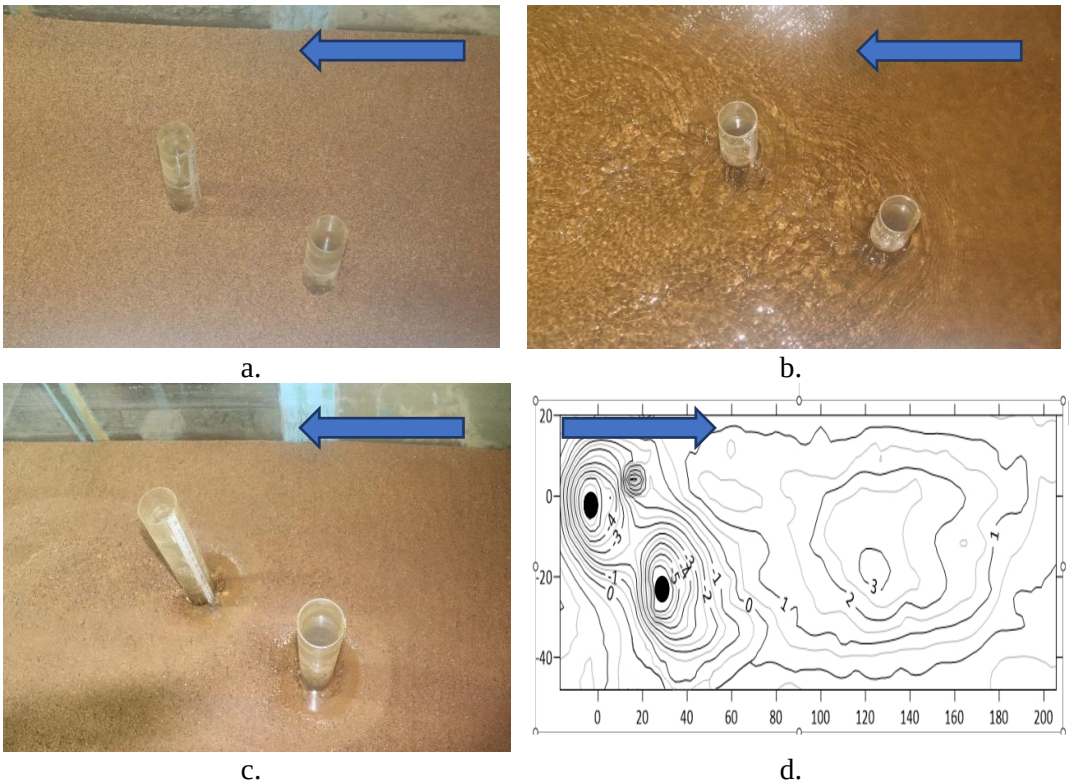

Fig 6.1.8 Experimental condition for experiment 8, *e* = 2.25*b*,a. Level bed, b. During Experiment, c. Scour bed, d. Contour Map.

The scour depth observed at the front pier was 0.1 m and that at the eccentric pier was 0.0111 m, after the completion of the experiment surfer software was used to generate contour maps.

6.1.9Experiment No. 9

This experiment was conducted for an eccentricity of 2.5*b* for 12 hours. The values of subsequent scour depths were recorded with a help of the laser distance meter.The frequency of recording the scour depths was incremented with the passing of each hour. It was observed that the maximum scour depth in this experiment was very close to the previous experiment i.e., *e*= 2.5 *b*.

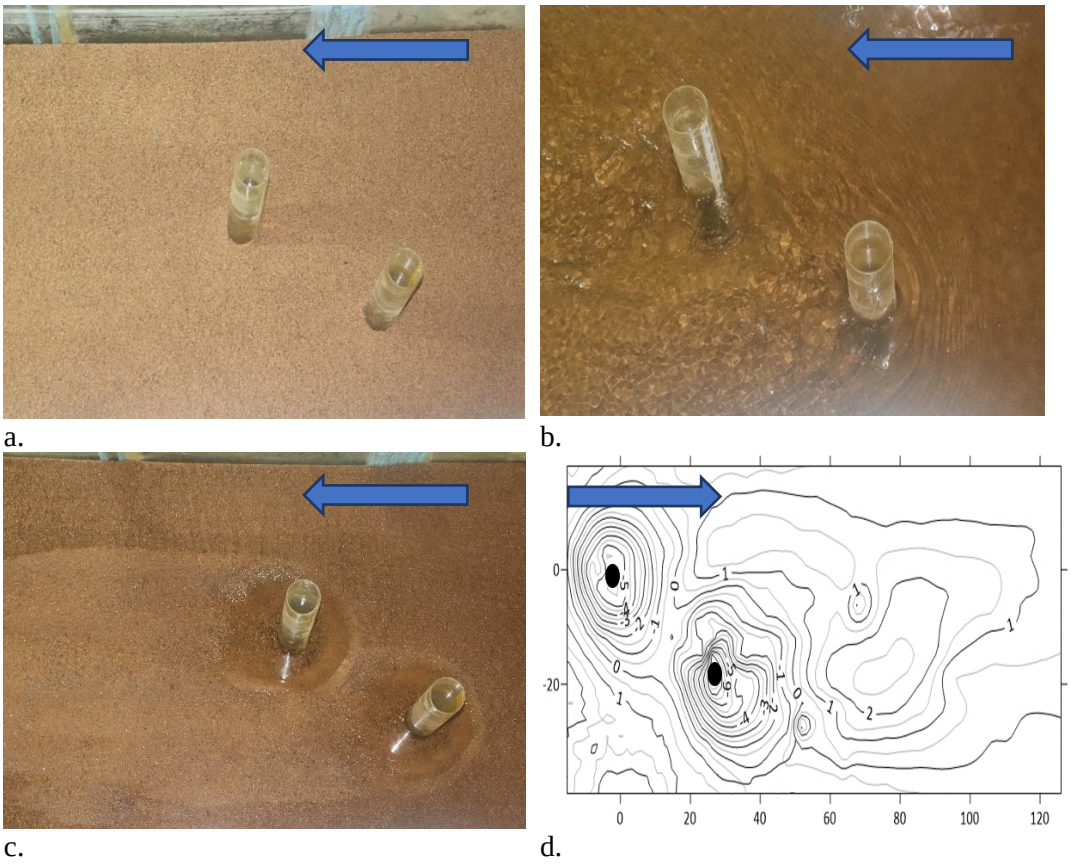

Fig 6.1.9 Experimental condition for experiment 9, *e* = 2.5*b*,a. Level bed, b. During Experiment, c. Scour bed, d. Contour Map.

The scour depth observed at the front pier was 0.09 m and that at the eccentric pier was 0.104 m, after the completion of the experiment.

6.1.10Experiment No. 10

This experiment was conducted for an eccentricity of 2.75*b* for 12 hours. The values of subsequent scour depths were recorded with a help of the laser distance meter.

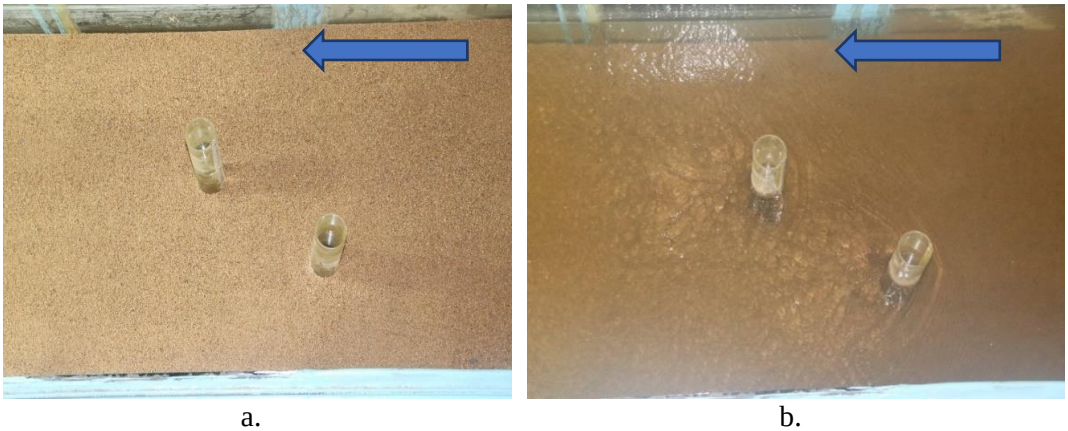

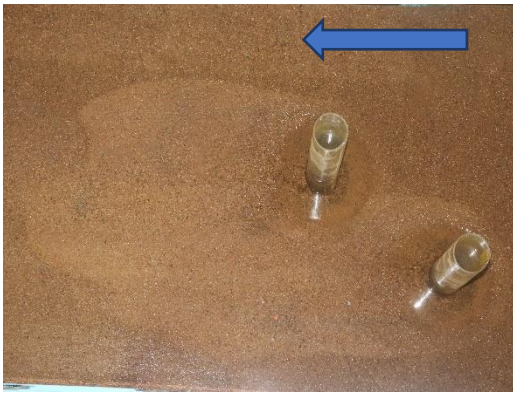

c.

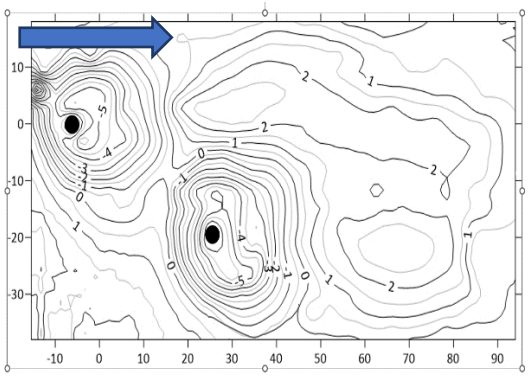

d.

Fig 6.1.10 Experimental condition for experiment 10, *e* = 2.75*b*,a. Level bed, b. During Experiment, c. Scour bed, d. Contour Map.

The frequency of recording the scour depths was incremented with the passing of each hour. The scour depth observed at the front pier was 0.079 m and that at the eccentric pier was 0.088 m, after the completion of the experiment.

6.1.11Experiment No. 11

This experiment was conducted for an eccentricity of 3*b* for 12 hours. The values of subsequent scour depths were recorded with a help of the laser distance meter.

a.

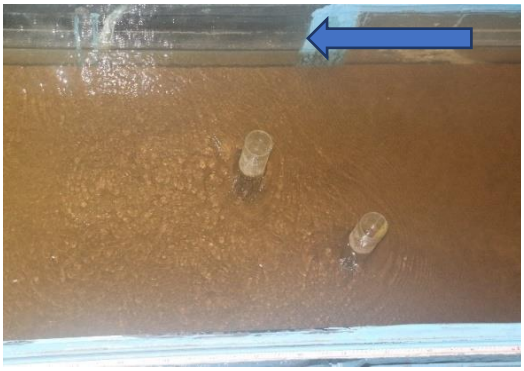

b.

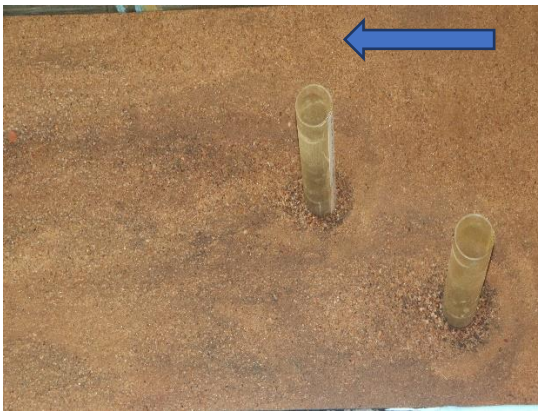

c.

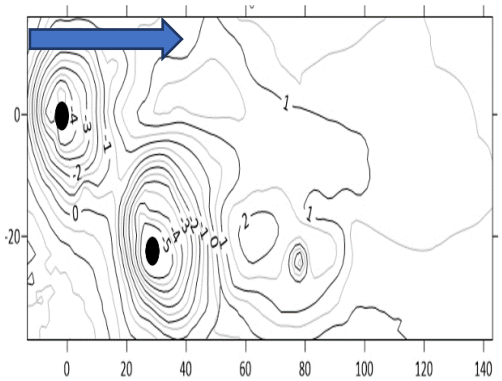

d.

Fig 6.1.11 Experimental condition for experiment 11, *e* = 3*b*,a. Level bed, b. During Experiment, c. Scour bed, d. Contour Map.

The frequency of recording the scour depths was incremented with the passing of each hour. The maximum scour depth observed at the front pier was 0.0753 m and that at the eccentric pier was 0.0935 m, after the completion of the experiment.

6.1.12Experiment No. 12

This experiment was conducted for an eccentricity of 3.5*b* for 12 hours. The values of subsequent scour depths were recorded with a help of the laser distance meter.

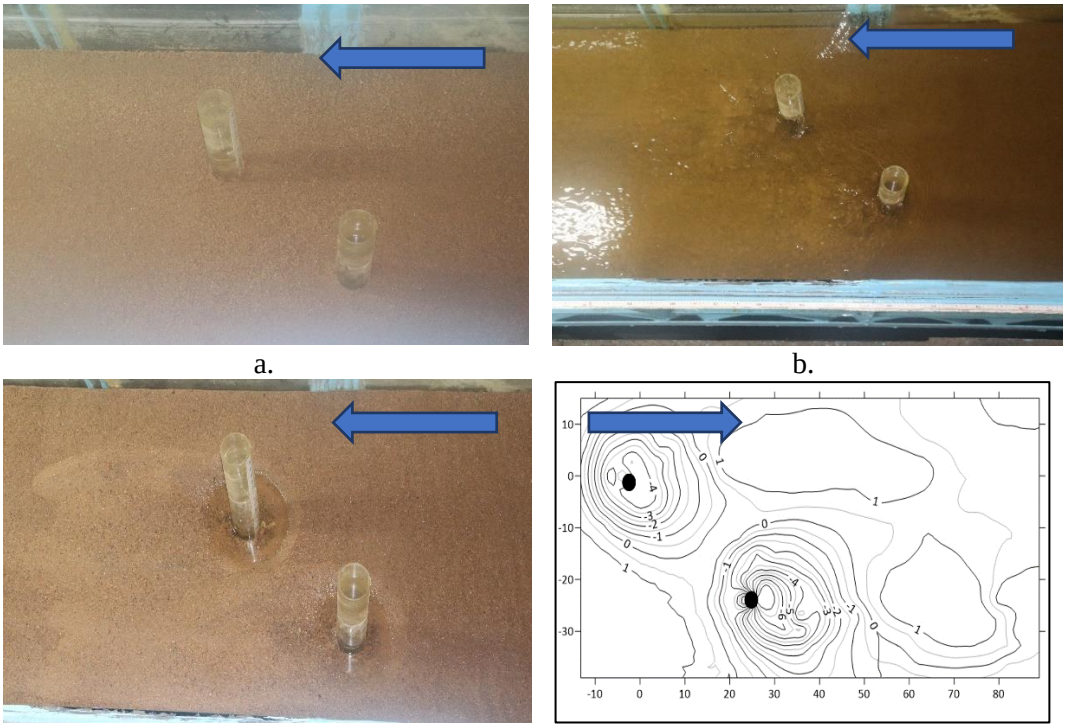

Fig 6.1.12 Experimental condition for experiment 12, e = 3.5b,a. Level bed, b. During Experiment, c. Scour bed, d. Contour Map.

The frequency of recording the scour depths was incremented with the passing of each hour. The maximum scour depth observed at the front pier was 0.079 m and that at the eccentric pier was 0.0859 m, after the completion of the experiment.

Table 6.2: Experimental outcomes

Experiment No	e (cm)	b (cm)	d_{sf}(cm)	d_{se} (cm)	l_s(cm)	w_s(cm)	a_{ps} (cm^2)	a_{ss} (cm^2)	V_s (cm^3)
1	2b	7	6.9	7.9	77.7	58.4	10196.7	10297.1	12514.3
2	2.25b	7	11.3	12.1	78.2	58.6	6014.6	6062.06	6767.9
3	2.5b	7	12.6	13.6	91.5	59.1	10236.3	10383.2	10236.3
4	2.75b	7	12.2	13.9	79.3	60.25	7931.3	8003.6	11819.4
5	3b	7	8.6	10.6	91.3	64.7	10435.1	10510.9	13284.8
6	3.5b	7	8.2	9.3	94.11	63.75	9367.7	9438.3	11330.4
7	2b	7	7.01	10.15	72.2	47.65	4894.1	4944.3	5438.5

8	2.25*b*	7	10.0	11.11	53.85	40.65	6467.3	6752.3	6978.2
9	2.5*b*	7	9.0	10.4	67.3	52.65	5604.06	5666.5	6209.1
10	2.75*b*	7	7.9	8.8	62.50	53.2	4366.5	4452.03	5727.4
11	3*b*	7	7.53	9.35	71.2	52.20	6256.0	6302.5	5276.5
12	3.5*b*	7	7.9	8.59	71.3	52.36	3592.3	3636.02	3168.1

6.1.13 Comparison of maximum scour depths between the front and eccentric piers

The maximum scour depth, which differs from the equilibrium scour depth, occurs after the experimental run. Our major goal is to examine the impacts of eccentricity on scour, hence experimental duration had reduced to 12 hours for all the experiments. Equilibrium scour depth occurs asymptotically with time, but theoretically, it will require infinite time to reach the equilibrium state.

In the first six experiments, the maximum scour depth was recorded after the experimental duration i.e.,12 hours. The inflow depth was maintained at 12.7 cm for theexperiments.

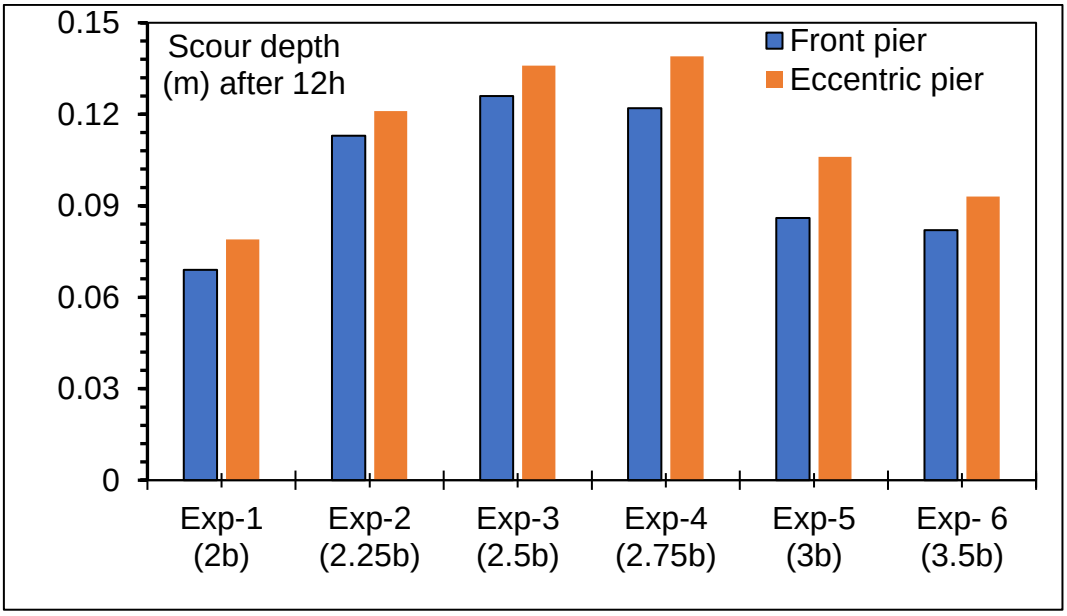

Fig 6.13a Maximum scour depth for first six experiments

The experiment with the eccentricity of 2*b* had the lowest maximum scour depth of any of the other experiments, whereas the experiment with the eccentricity of 2.75*b* had the highest maximum scour depth.

In the rest six experiments, the maximum scour depth was recorded after the experimental duration i.e.,12 hours. The inflow depth was maintained at 13.7 cm for theexperiments clearly shown in**Fig 6.13a**.

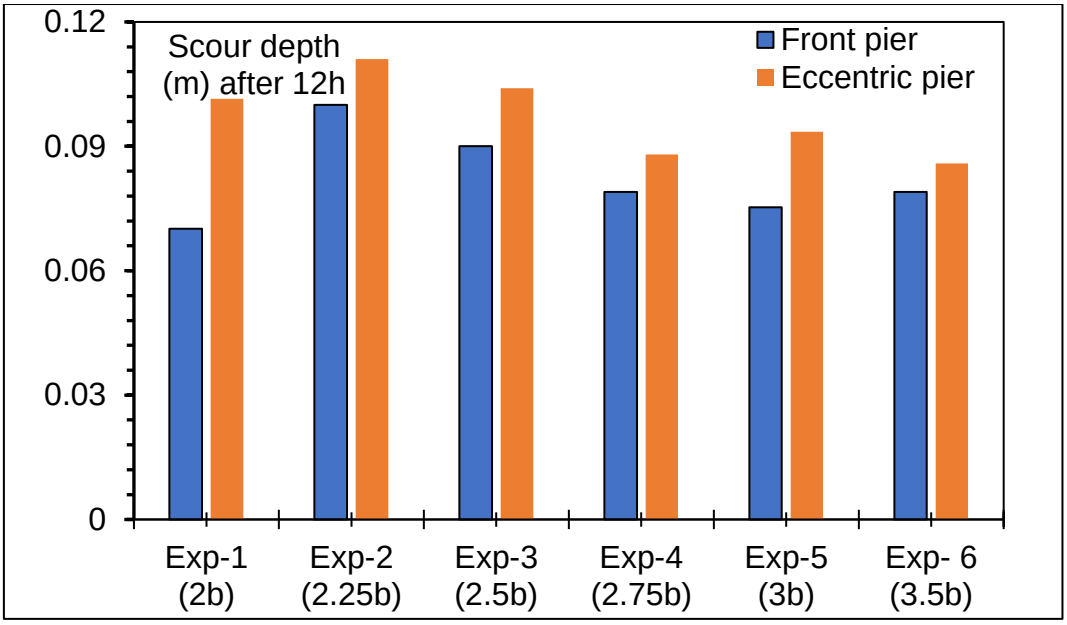

Fig 6.13b Maximum scour depth for next six experiments

The experiment with the eccentricity of 2.75*b* had the minimum scour depth, whereas the experiment with the eccentricity of 2.25*b* had the lowest maximum scour depth of any of the other experiments shown in **Fig 6.13b**.

6.1.14 Temporal evolution of scour depth

The evolution of instantons scour depth was measured physically with the help of a disto-meter, after applying the refraction correction factor. It was observed that the 70-80 % scour occurred in the first 3-4 hours, which can be seen from the time vs depth graph. For all the experiments, it was clearly seen that the rate of scour development is higher for eccentric piers due to the combined effect of the wake vortex of the upstream pier and the horseshoe vortex of the downstream pier generally known as the interference effect. The time-dependent scour depth for all the 12 experiments is shown in **Figs 6.14–6.25**.

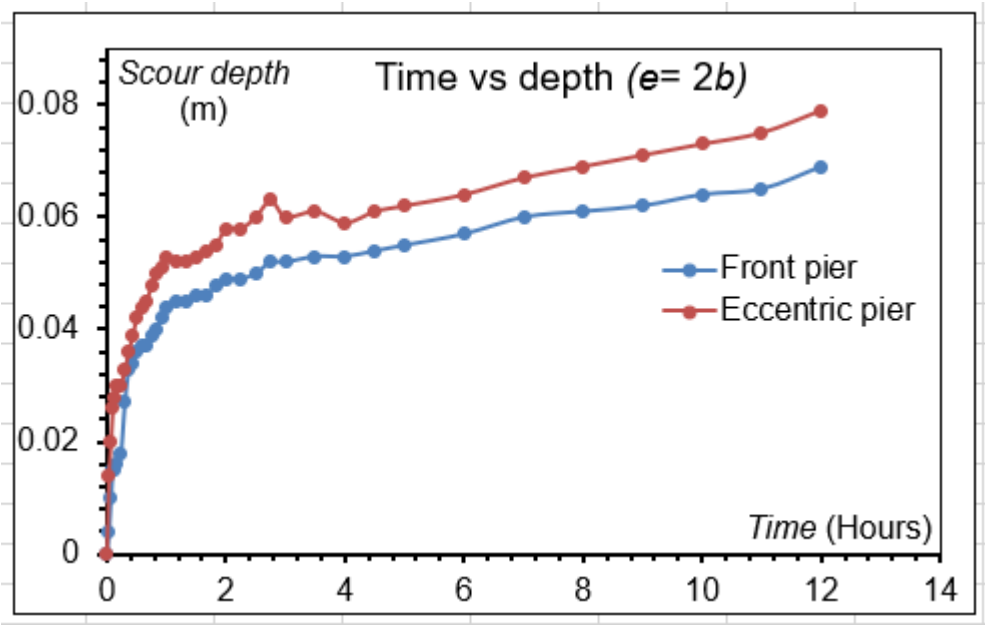

Fig. 6.14 Temporal evolution of scour during experiment -1

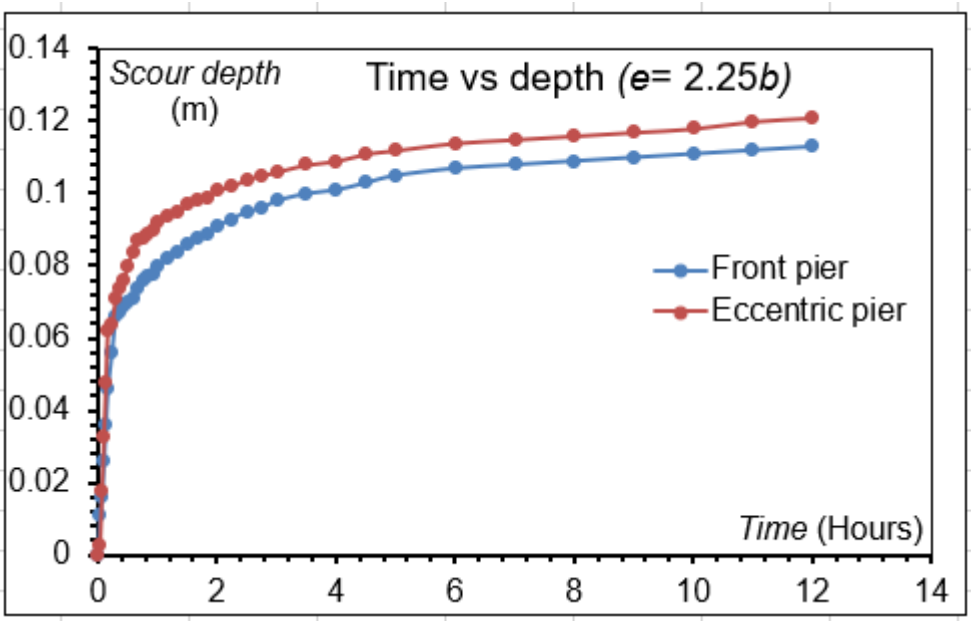

Fig. 6.15 Temporal evolution of scour during experiment -2

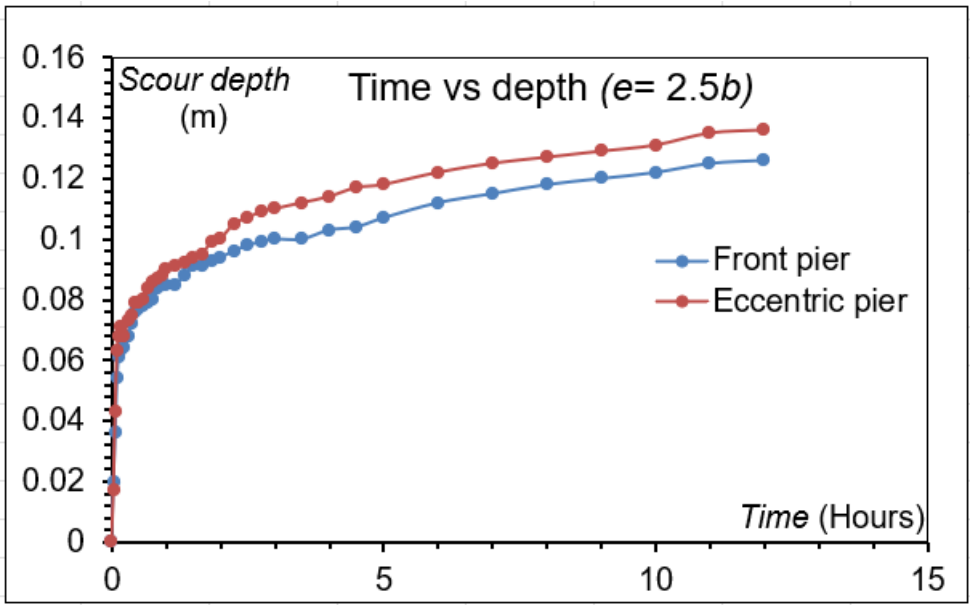

Fig. 6.16 Temporal evolution of scour during experiment -3

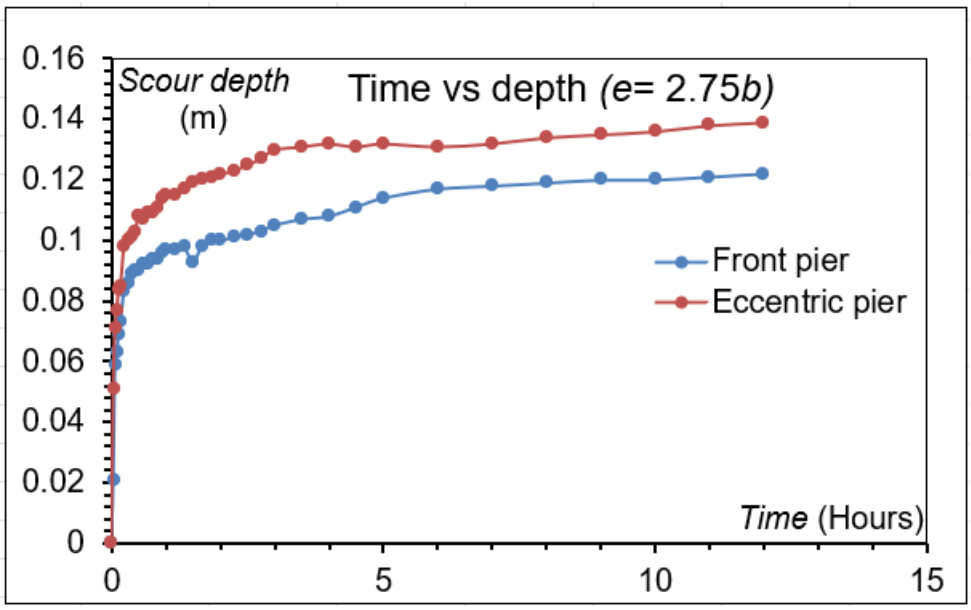

Fig. 6.17 Temporal evolution of scour during experiment -4

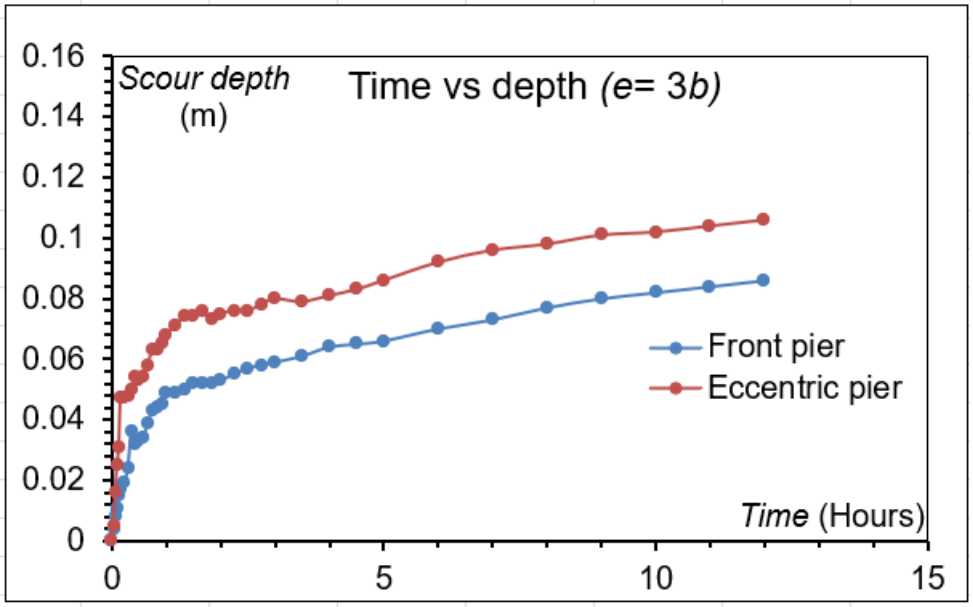

Fig. 6.18 Temporal evolution of scour during experiment -5

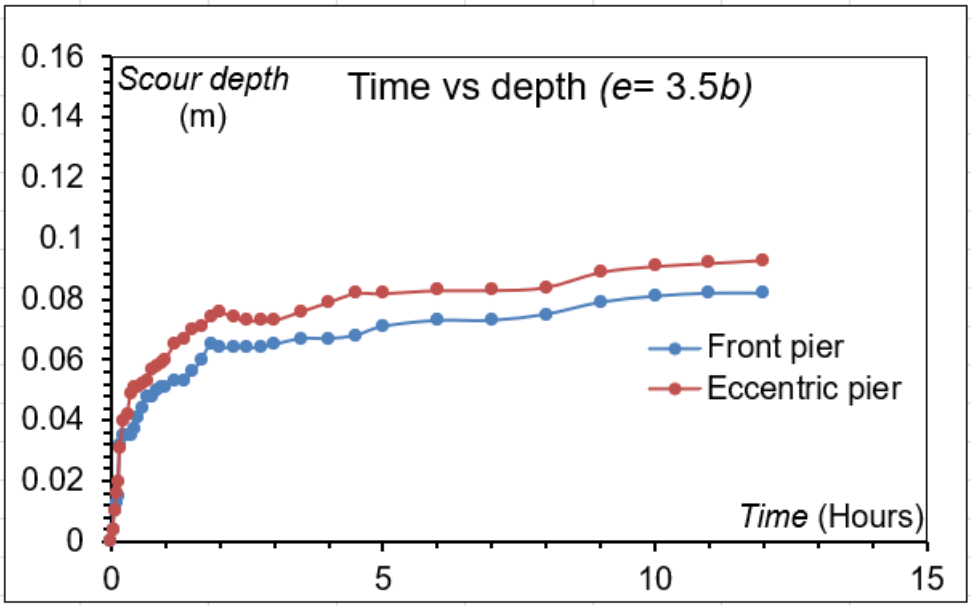

Fig. 6.19 Temporal evolution of scour during experiment -6

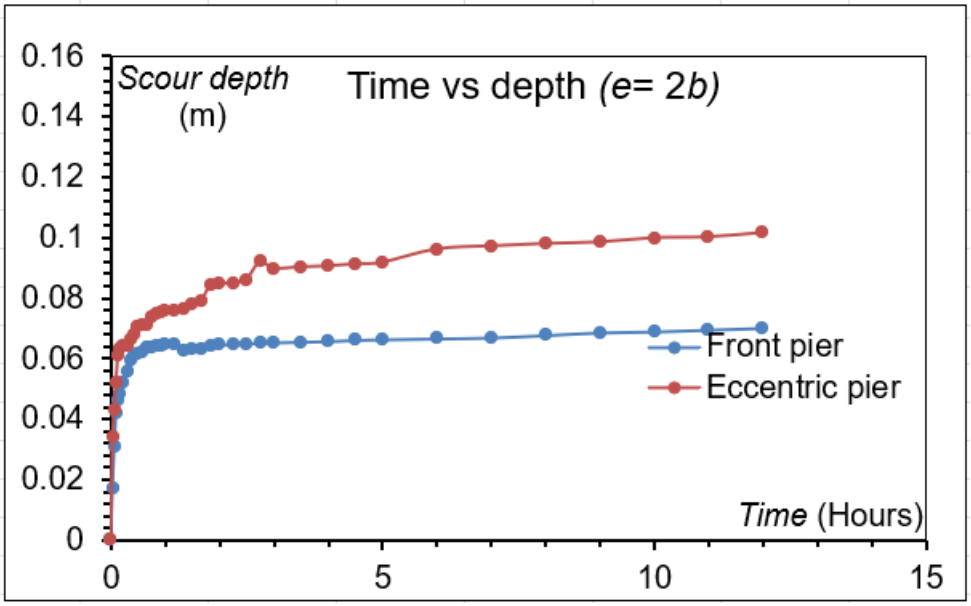

Fig. 6.20 Temporal evolution of scour during experiment -7

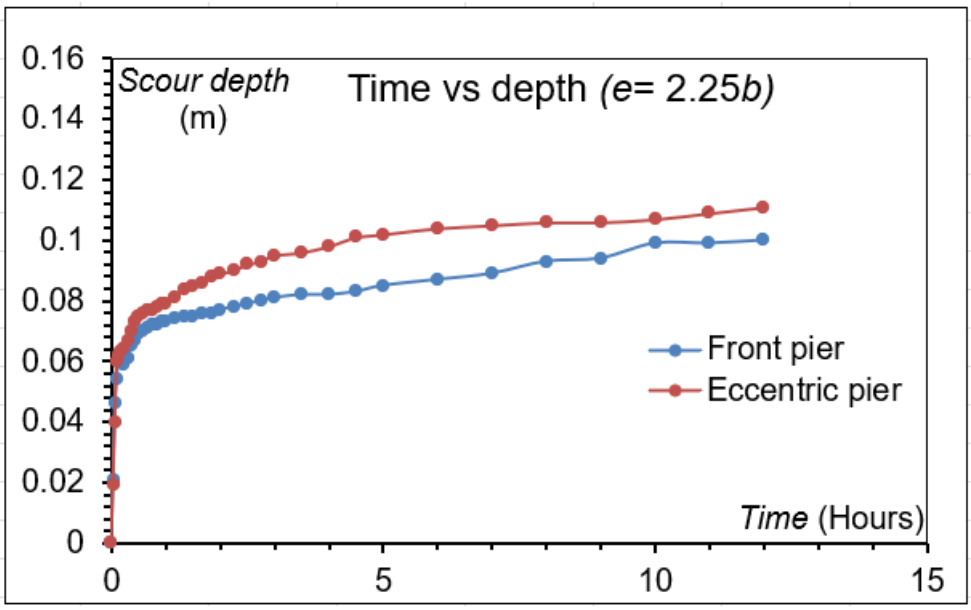

Fig. 6.21 Temporal evolution of scour during experiment -8

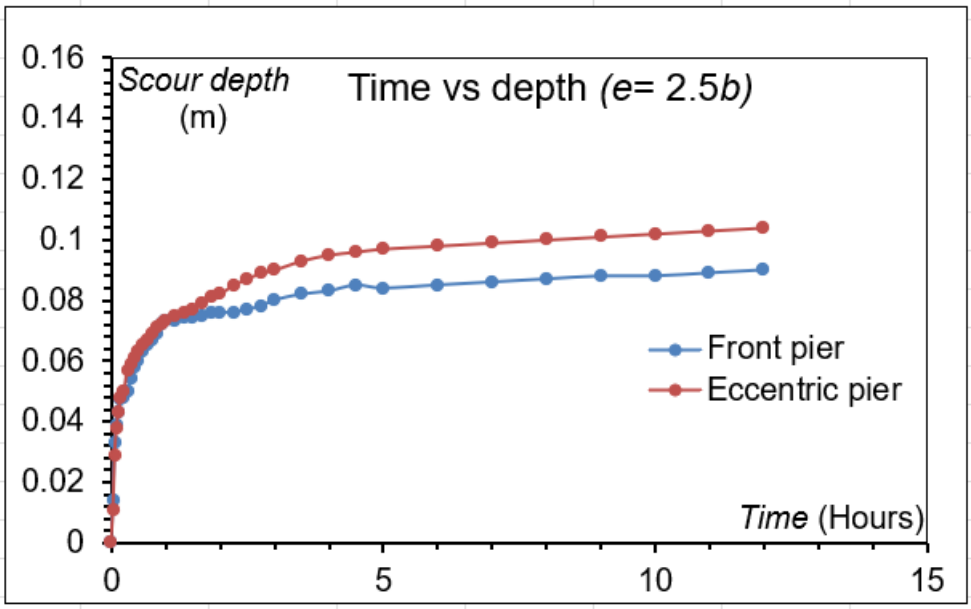

Fig. 6.22 Temporal evolution of scour during experiment -9

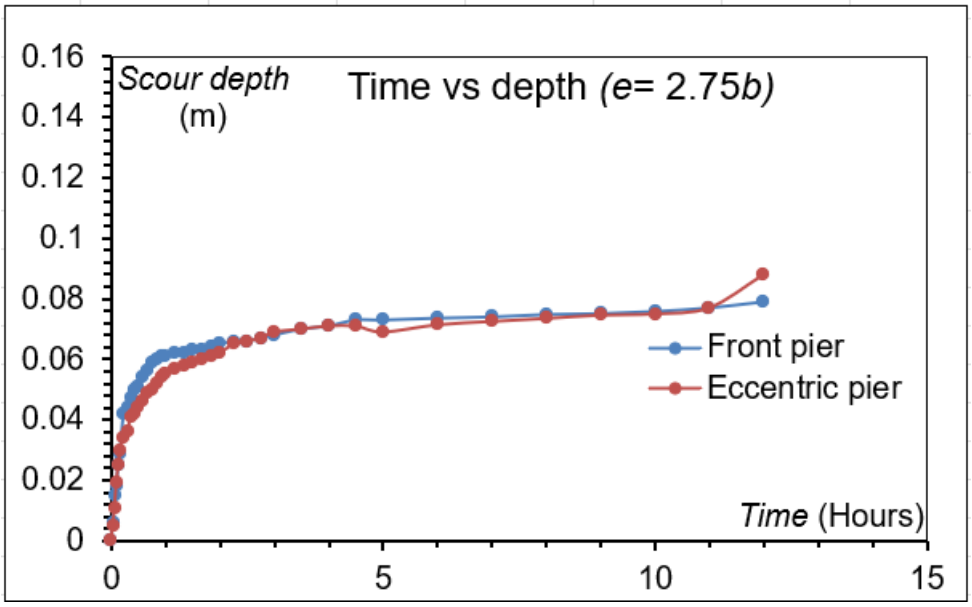

Fig. 6.23 Temporal evolution of scour during experiment -10

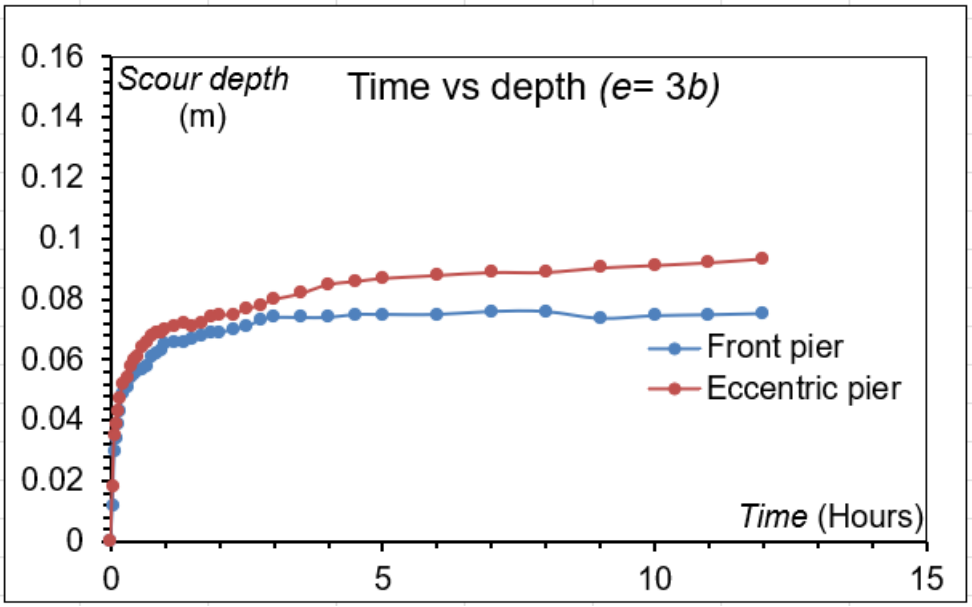

Fig. 6.24 Temporal evolution of scour during experiment -11

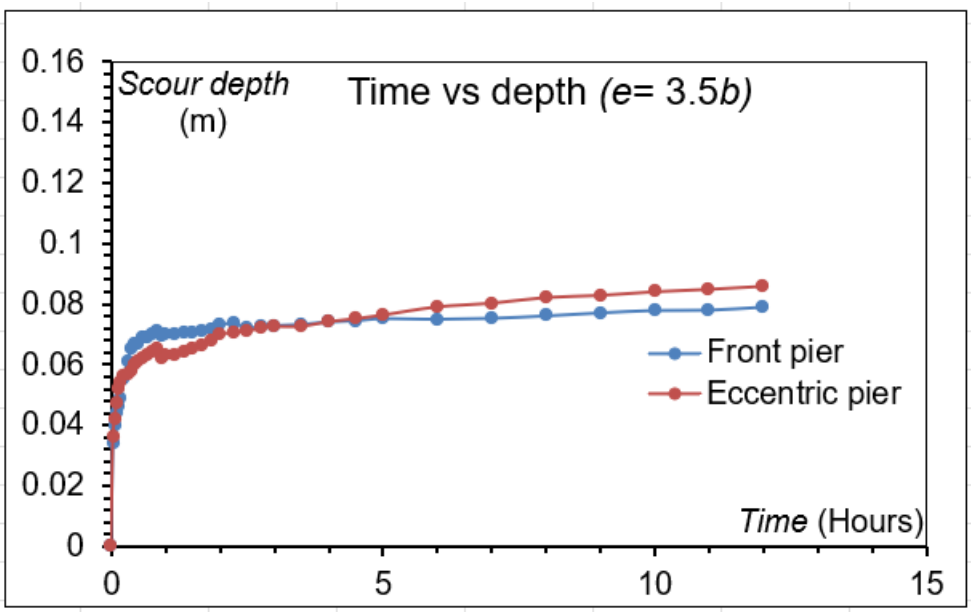

Fig. 6.25 Temporal evolution of scour during experiment -12

6.1.15Variation of plane surface area with varying eccentricity

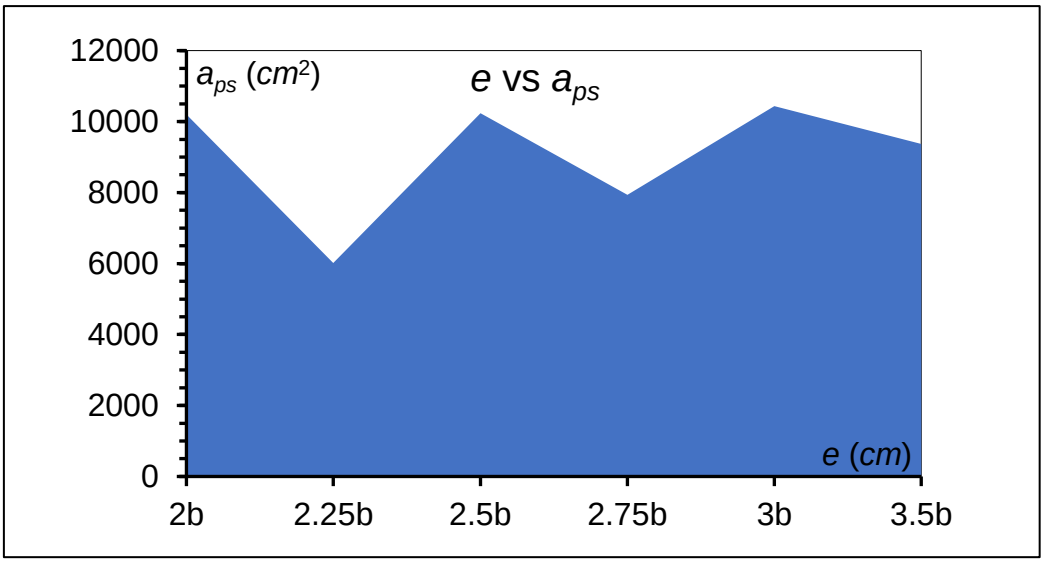

Fig. 6.26 Plane surface area(a_{ps}) at different eccentricities for h=12.7 cm

During the 12 hours of experimental run for the first six experiments, inflow depth was kept fixed at 12.7 cm. And after completing the procedure, from the experimental data, the plane surface area (a_{ps}) for each eccentricity was calculated with the help of Surfer software. From **Fig.6.26,** we can observe that the plane surface area is found to be the highest for the eccentricity e=3b and the lowest for the eccentricity e=2.25b.

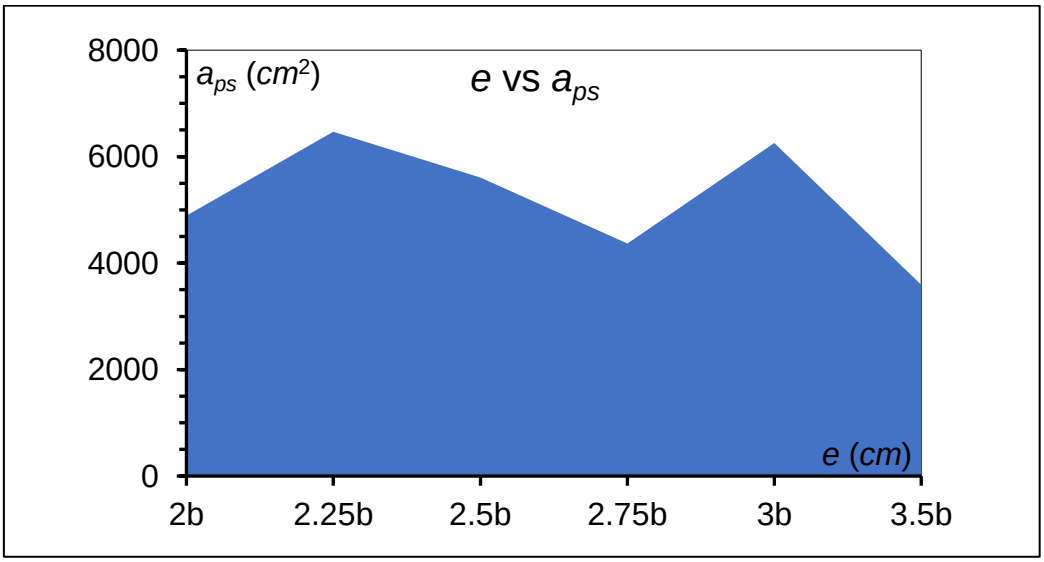

Fig. 6.27 Plane surface area (a_{ps}) at different eccentricities for h= 13.7 cm

During the 12 hours of experimental run for the next six experiments, inflow depth was kept fixed at 13.7 cm. And after completing the procedure, from the experimental data, the plane surface area (a_{ps}) for each eccentricity was calculated with the help of Surfer software. From **Fig.6.27,** we can observe that the plane surface area is found to be the highest for the eccentricity e=2.25b and the lowest for the eccentricity e=3.5b.

6.1.16Variation of scour surface area with varying eccentricity

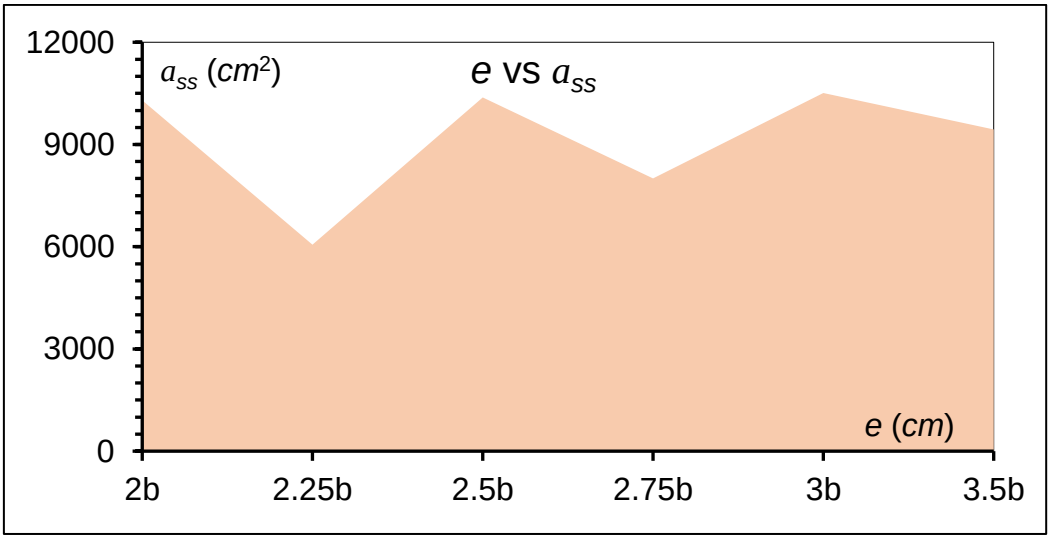

Fig. 6.28 Variation of surface area of scour (a_{ss}) with varying eccentricity for h= 12.7 cm

During the 12 hours of experimental run for the first six experiments, inflow depth was kept fixed at 12.7cm.And after completing the procedure, from the experimental data, the surface area of scour (a_{ss}) for each eccentricity was calculated with the help of Surfer software.From **Fig.6.28,** we can observe that the surface area of scour is found to be the highest for the eccentricity e=3.5b and the lowest for the eccentricity e=2.25b.

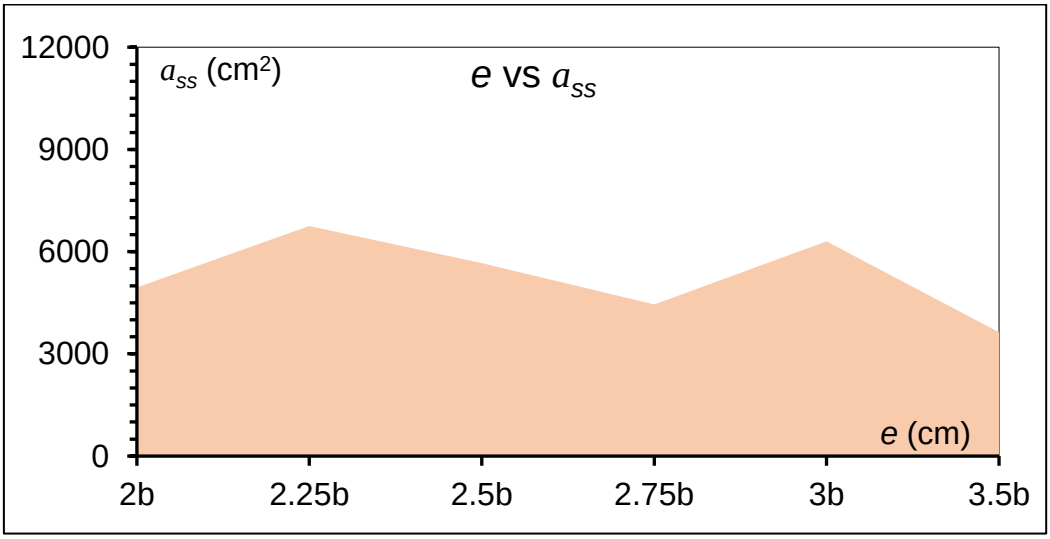

Fig. 6.29 Variation of surface area of scour (a_{ss}) with varying eccentricity for h= 13.7 cm

During the 12 hours of experimental run for the lastsix experiments, inflow depth was kept constant at 13.7cm. After completing the procedure, from the experimental data,the surface area of scour (a_{ss}) for each eccentricity was calculated with the help of Surfer software. From **Fig.6.29,** we can see that the surface area of scour is foundto be the highest for eccentricity e=2.25b and the lowest for eccentricity e=3.5b.

6.1.17Variation of scour volume with varyingeccentricity

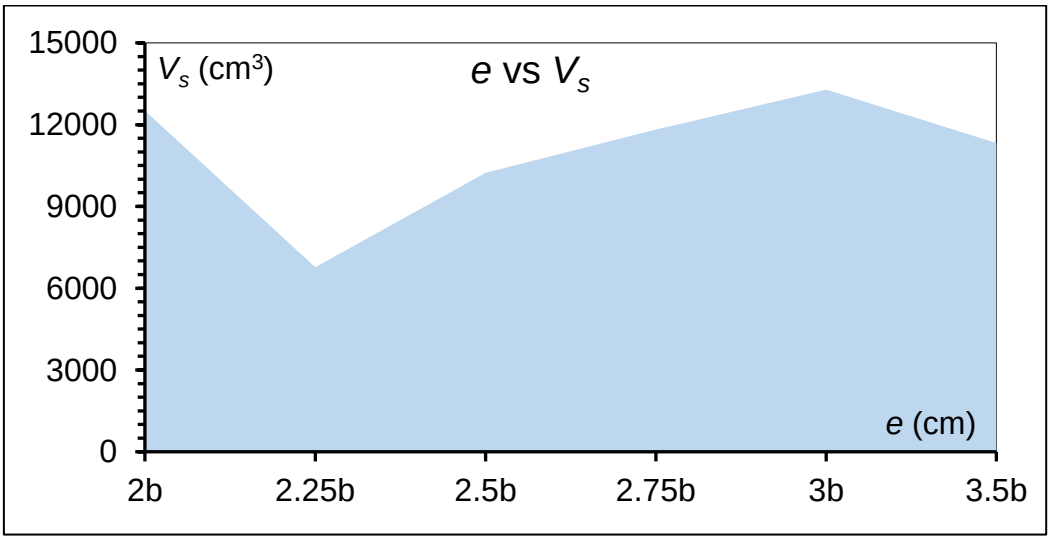

Fig. 6.30 Change of scour volume at different eccentricity for h= 12.7 cm

During the 12 hours of experimental run for the first 6 series of experiments inflow depth was kept 12. 7cm.And after completing the procedure from the experimental data volumeof scour (v_s) for each eccentricity was calculated with the help of surfersoftware. And from **Fig.6.30,** we can see thatthe volume of scour(v_s) is found to be highest foreccentricity e=3b and lowest for eccentricity e=2.25b.

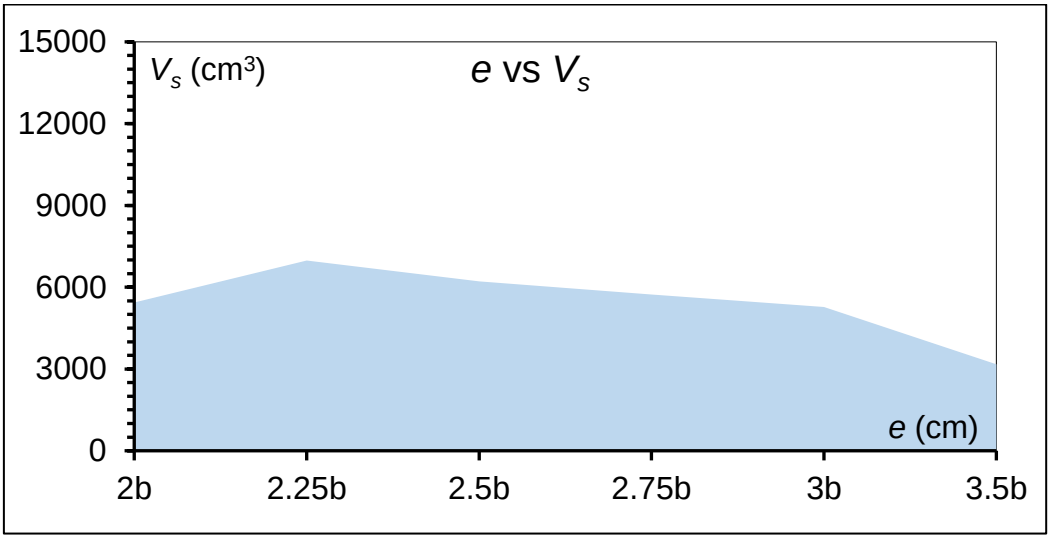

Fig. 6.31 Change of scour volume at different eccentricity for h= 13.7 cm

During the 12 hours of experimental run for the last 6 series of experiments, inflow depth was kept constant at 13. 7cm.And after completing the procedure from the experimental data volume of scour (v_s) for each eccentricity was calculated with the help of surfer software. And from **Fig.6.31,** we can see that the volume of scour (v_s) is found to be highest for eccentricity e=2.25b and lowest for eccentricity e=3.5b

6.1.18Variation of scour width with varying eccentricity

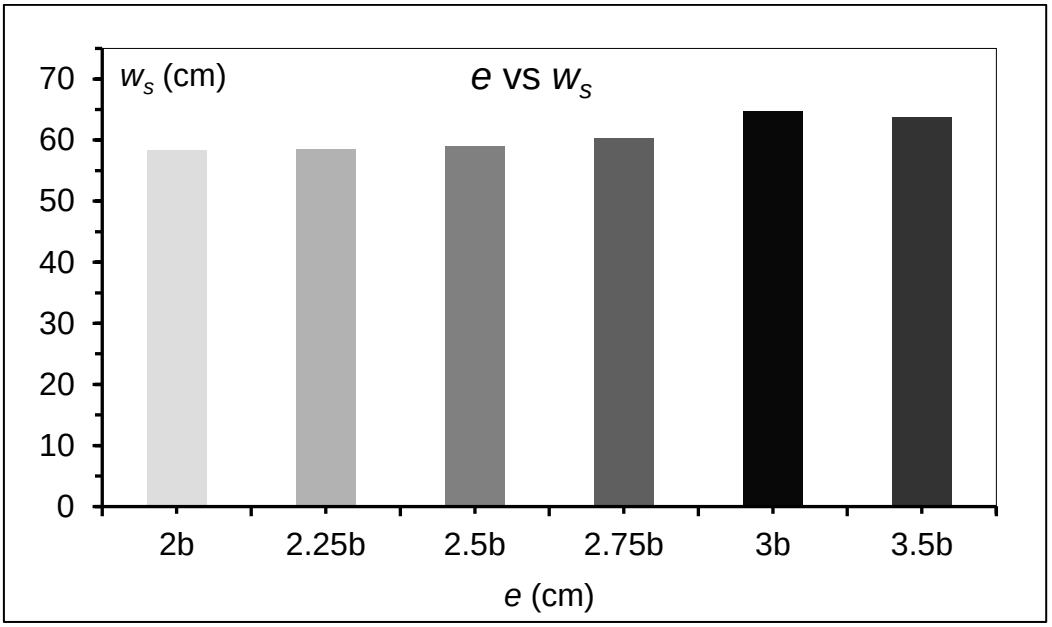

Fig. 6.33 Change of scour width at different eccentricities for h=12.7 cm.

During the 12 hours of experimental run for the first 6 series of experiments, inflow depth was kept fixed at 12.7cm.And after completing the procedure, from the experimental data,contour diagrams for each eccentricity weregenerated with the help of Surfer software.After getting all the contour diagramswith the help of surfer tools the width of scour (w_s)for each eccentricity was calculated. And from **Fig.6.33,** we can observe that the width of scour (w_s)was found to be highest for eccentricity e=3b and lowest for eccentricity e=2b.

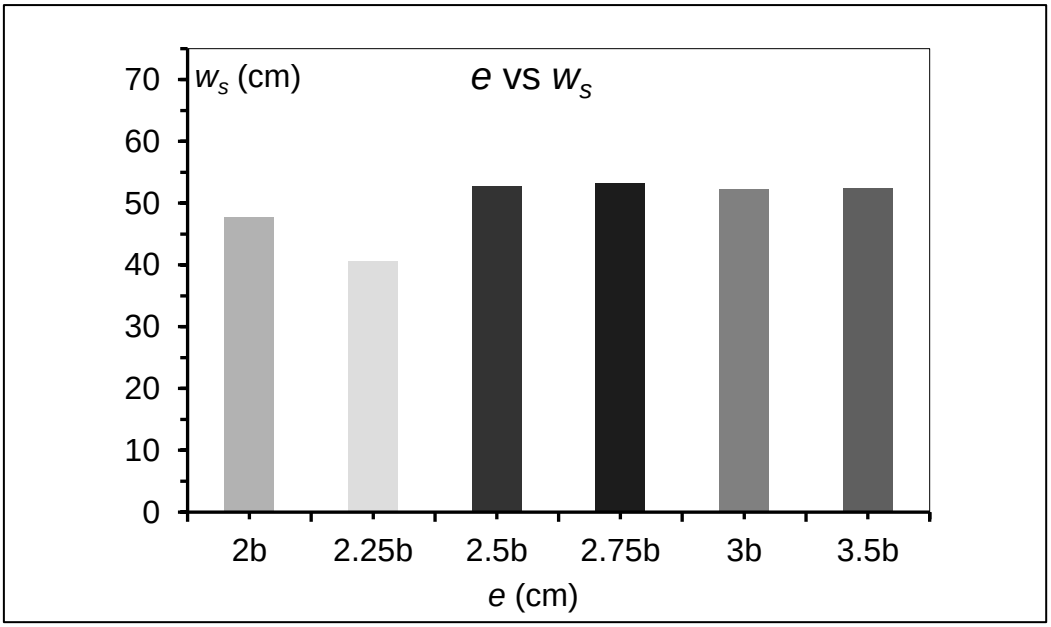

Fig. 6.34 Change of scour width at different eccentricity for h=13.7 cm.

During the 12 hours of experimental run for the last 6 series of experiments, inflow depth was kept at 13.7cm.And after completing the procedure, from the experimental data, contour diagrams for each eccentricity were generated with

the help of surfer software. After getting all the contour diagrams with the help of surfer tools the width of scour (w_s) for each eccentricity was calculated. And from **Fig.6.34,** we can observe that the width of scour (w_s) was found to be highest for eccentricity e=2.5b and lowest for eccentricity e=2.25b.

6.1.19Variation of scourlength with varying eccentricity

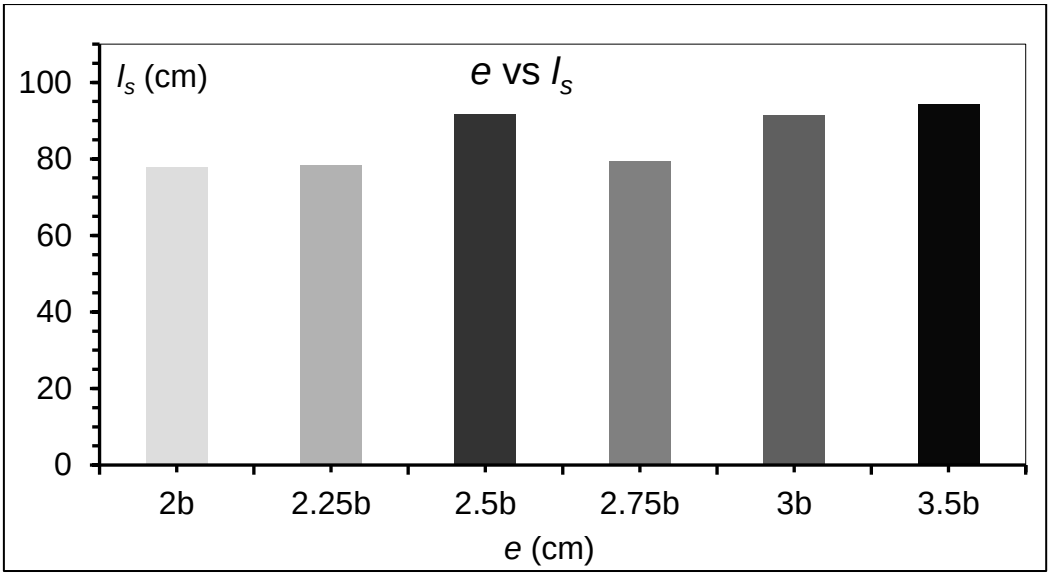

Fig. 6.35 Measuredscour length at different eccentricities for h=12.7 cm.

During the 12 hours of experimental run for the first 6 series of experiments, inflow depth was kept at 12. 7cm.And after completing the procedure, from the experimental data, contour diagrams for each eccentricity were generated with the help of surfersoftware. After getting all the contour diagrams with the help of Surfer tools the length of scour (l_s)for each eccentricity was calculated. And from **Fig.6.35,** we can see that the length of scour (l_s)was found to be highestfor eccentricity e=3.5b and lowest for eccentricity e=2b.

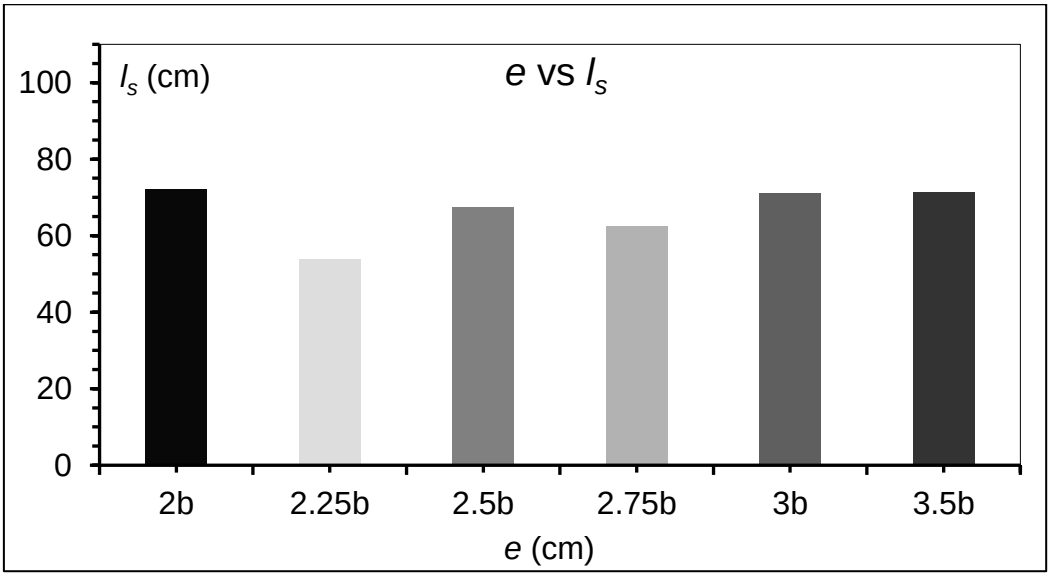

Fig. 6.36 Measured scour length at different eccentricities for h=13.7 cm.

During the 12 hours of experimental run for the last 6 series of experiments, inflow depth was kept constant at 13.7cm.And after completing the procedure, from the experimental data, contour diagrams for each eccentricity were generated with the help of surfer software. After getting all the contour diagrams with the help of surfer tools the length of scour (l_s) for each eccentricity was calculated. And from **Fig.6.36,** we can see that the length of scour (l_s) was found to be highest for eccentricity e=2b and lowest for eccentricity e=2.25b.

Chapter 7

7.1 Conclusions

Local scour around eccentric bridge piers in an alluvial channel is a complicated problem, with relatively little success in modelling the local scour computationally. As a result, the physical model remains the most effective method for estimating local scour depth. The physical model data demonstrate that eccentricity (*e*) and pier geometrymodel have a significant impact on local scour around the eccentric piers. The inline and eccentric spacing of the pier can make a significant difference in reducing the local scour depth.

The maximum scour depth around two circular piers, positioned in eccentric arrangement, is determined by carrying out12numbers of clear water scour experiments. And here for the first six experiments,the inflow depth was kept constant at 12.7cm with varying eccentric spacing from 2, 2.25, 2.5, 2.75,3 and 3.5 times the pier diameter (*b*). At *e*=2.75*b*, the maximum scour depth at the eccentric rear pier is found about 76% greater than that in the case of *e* =2*b*. The pier arrangement and the interference between the horseshoe vortex of the rear pier and the wake vortex of the front pier may also play an important role in the creation and formation of the greater scour depth at the eccentric rear piers. In addition, at *e*=2.5*b*, the maximum depth of the scour hole at the upstream or in-line front pier is about 82.5% more than that in the case of eccentricity *e* = 2*b*, which produces minimum scour depth in both cases. Also, maximum scour area and scour volume was obtained in case of eccentricity *e* = 3*b*.

And for the next 6 experiments, the inflow depth was kept constant at 13.7cm with the varying eccentric spacing from 2, 2.25, 2.5, 2.75,3 and 3.5 times the pier diameter (*b*). At *e*=2.25*b*, the maximum scour depth at the eccentric rear pier is found about 29% greater than that in the case of *e* =3.5*b*. The pier arrangement and the interference between the horseshoe vortex of the rear pier and the wake vortex of the front pier may also play an important role in the creation and formation of the greater scour depth at the eccentric rear piers. In addition, at *e*= 2.25*b*, the maximum depth of the scour hole at the upstream or in-line front pier is about 42.5% more than that in the case of eccentricity *e* = 2*b*, which produces minimum scour depth in both cases. Also, maximum scour area and scour volume was obtained in case of eccentricity *e* = 2.25*b*.

The maximum scour occurrence phenomenon in terms of different scour parametersmay be used to shift sediment towards the channel bank in the real field.On the other way, the minimum scour occurrence criteria may be used for the economic and safe design bridge pier.

A limitation of the present study is that as all the experiments were conducted on a small laboratory scale and it was a model study so it may differ from the actual results.

7.2 Future scope of the study

In the current study scour depth data was analyzed by keeping the inflow depth constantand by varying eccentricity for two different inflow depths. Further analysis can be done by varying the eccentricity along with the inflow depth and vice versa. More studies can be done based on the variation of longitudinal inline spacing along with eccentricity. Because a bridge pier can be built on soil other than cohesion-less soil, analyzing the performance of a collar as well as the temporal development of scour in cohesive soil will provide useful insight into the behaviour of a collar in this situation.Scour can be reduced by using collars. Collars are not only excellent at reducing scour, but they are also far less expensive when compared to countermeasure measures such as riprap. It should also be noted that utilizing a collar induced a delay in the scouring mechanism, and increasing the size of the collar increased the delay time. As the pier spacing grows, the region between the piers without protection is washed away, resulting in greater scour holes at the back piers.

7.3 References

Abed, L. and Gasser M. M., (1993). Model study of local scour downstream bridge piers. Proceedings National Conf. on Hydraulic Engineering, San Francisco, 1738–1743.

Ahmed, F., & Rajaratnam, N. (1998). Flow around bridge piers. *Journal of Hydraulic Engineering*, *124*(3), 288-300.

Ashtiani B. A. and. Kordkandi A. A, (2012). Flow field side-by-side piers with and scour without hole. *European Journal of Mechanics B/Fluilds*, Vol. 36, pp.152-166.

Barbhuiya A.K., Dey, Measurement of turbulent flow field at a vertical semi-circular cylinder attached to the sidewall of a rectangular channel (2004) Flow *Measurement and Instrumentation*, 15 (2), pp. 87-96.

Breusers, H. N. C., Nicollet, G., & Shen, H. W. (1977). Local scour around cylindrical piers. *Journal of Hydraulic Research*, 15(3), 211-252.

Breusers, H.N.C. and Raudkivi, A.J. (1991). Scouring. IAHR hydraulic structures design manual, Rotterdam, The Netherlands, 2.

Barbhuiya, A.K. and Dey, S. (2004). Local scour at abutments: a review, Sadhana. *Proc. Indian Acad. Sci.*, 29(Oct.), pp. 449-476.

Cheremisinoff, N. P., & Cheremisinoff, P. N. (1987). *Flow Measurement for Engineers and Scientists* (Vol. 32). CRC Press.

Chiew, Y. M. &Lim, F. H., (2001). Parametric study of riprap failure around bridge piers. *Journal of hydraulic research*, 39(1), 61-72.

Das, S., Das, R. andMazumdar, A. (2013). Comparison of characteristics of horseshoe vortex at circular and square piers. *Research Journal of Applied Sciences, Engineering and Technology*, 5(17), pp. 4373-4387.

Dargahi, B. (1990). Controlling Mechanism of local scouring. *Journal of Hydraulic Engineering*, 116(10), pp. 1197-1214.

Das, S., Ghosh, S. and Mazumdar, A. (2014). Kinematics of Horseshoe Vortex in a Scour Hole around Two Eccentric Triangular Piers. *International Journal of Fluid Mechanics Research*, 41(4), pp. 296-317.

Das, S. and Mazumdar, A. (2015). Turbulence flow field around two eccentric circular piers in scour hole. *International Journal of River Basin Management*, 13(3), pp. 343-361

Das, S., Das, R., & Mazumdar, A. (2015). Velocity profile measurement technique for scour using ADV. In *Proceedings of the 2015 International Conference on Testing and Measurement: Techniques and Applications, TMTA* (pp. 249-252).

Das, R., Das, S., Jaman, H. and Mazumdar, A. (2019). Impact of Upstream Bridge Pier on the Scouring Around Adjacent Downstream Bridge Pier. *Arabian Journal for Science and Engineering*, 44(5), pp. 4359–4372

Dey, S., Bose, S. K. and Sastry, G.L.N. (1995). Clear Water Scour at Circular Piers. *Journal of Hydraulic Engineering*, 121(12), pp. 869-876.

Dey, S. (1999). Time-variation of scour in the vicinity of circular piers. *Proceedings of the Institution of Civil Engineers-Water Maritime and Energy*, 136(2), 67-75.

Dey, S. (2003). Incipient Motion of Bivalve Shells on Sand Beds. *Journal of Engineering Mechanics*, 129 (2), 232-240.

Dey, S., & Raikar, R. V. (2007). Characteristics of horseshoe vortex in developing scour holes at piers. *Journal of Hydraulic Engineering*, 133(4), 399-413.

Dey, S. and Barbhuiya, A.K. (2005). Turbulent flow field in a scour hole at a semicircularabutment. *Canadian Journal of Civil Engineering*, 32(1), pp. 213-232.

Graf, W.H. and Istiarto, I. (2002). Flow pattern in the scour hole around a cylinder. *Journal of Hydraulic Research*, 40(1), pp. 13-20.

Hoffmans, G. J., & Verheij, H. J. (1997). *Scour manual*. Routledge.

Jain, S.C. and Fischer, E.E. (1979). Scour around bridge piers at high Froude numbers. Report. No. FHWA- RD-79-104, Federal Highway Administration. Washington D.C

Jaman, H, Das, S., Kuila, A. and Mazumdar, A. (2017*a*). Hydrodynamic flow patterns around three inline eccentrically arranged circular piers. *Arabian Journal for Science and Engineering*, 42(9), pp. 3973-3990.

Jaman, H., Das, S., Das, R. and Mazumdar, A. (2017*b*). Hydrodynamics of flow obstructed by inline and eccentrically-arranged circular piers on a horizontal bed surface. *Journal of The Institution of Engineers (India): Series A*, 98(1-2), pp. 77-83.

Khaple, S., Hanmaiahgari, P.R., Gaudio, R. and Dey, S. (2017). Interference of an upstream pier on local scour at downstream piers. *Acta Geophysica*, 65(1), pp. 29-46.

Kothyari, U.C., Raju, K.G.R. and Garde, R.J. (1992*a*). Live-bed scour around cylindrical bridge piers. *Journal of Hydraulic Research*, 30(5), pp. 701-715.

Kothyari, U.C., Raju, K.G.R. and Garde, R.J. (1992*b*). Temporal variation of scour around circular bridge piers. *Journal of Hydraulic Engineering*, 118(8), pp.1091-1106.

Kothyari U. C. and Ranga Raju K. G. (2001) Scour around spur dikes and bridgeabutments, *JournalofHydraulicResearch*, 39(4), pp. 367-374,

Liu, H. K., Chang, F. M. and Skinner, M. M. (1961). Effect of bridgeconstriction on scour and backwater. Report No. CER60HKL22, Civil Engineering Section, Colorado State Univ. Fort Collins, Colo.

Laursen,E.M.andToch,A.(1956).Scouraroundbridgepiersandabutments.
Vol.4.IowaHighwayResearchBoard.Ames,Iowa.

Larson, T. D. (1991). Highway Statistics 1990 (No. FHWA-PL-91-003). United States. Federal Highway Administration.

Link, O., & Zanke, U. (2004). On the time-dependent scour-hole volume evolution at a circular pier in uniform coarse sand. In *Proceedings 2nd*

International Conference on Scour and Erosion (ICSE-2). November 14.–17., 2004, Singapore.

Marsh, N.K., Western, A.W. and Grayson, R.B. (2004). Comparison of methods for predicting incipient motion for sand beds. *Journal of Hydraulic Engineering*, 130(7), pp. 616-621.

Melville, B.W. (1975). Local scour at bridge sites. Rep. No. 117, School of Engineering, University of Auckland, Auckland, New Zealand.

Melville, B. and Sutherland, A. (1988). Design method of time Dependent Local ScouratCircularBridgePier.*JournalofHydraulicEngineering*,114(10),pp.1210-1226.

Muzzammil, M. and Gangadhariah, T. (2003). The mean characteristics of horseshoe vortex at a cylindrical pier. *Journal of Hydraulic Research*, 41(3), pp. 285-297.

Melville, B.W. (1975). Local scour at bridge sites. Rep. No. 117, School of Engineering, University of Auckland, Auckland, New Zealand.

Melville, B.W. (1992). Local scour at bridge abutments. *Journal of Hydraulic Engineering*, 118(4), pp. 615–631.

Melville, B.W. and Chiew, Y.M. (1999). Time scale for local scour at bridge piers. *Journal Hydraulic Engineering*, 125(1), pp. 59-65.

Melville, B.W. and Coleman, S.E. (2000). Bridge scour. Water Resources Publications, Fort Collins, Colorado, USA.

Oliveto, G. and Hager, W.H. (2002). Temporal evolution of clear-water pier and abutment scour. *Journal of Hydraulic Engineering*, 128(9), pp. 811-820.

Raudkivi, A. J., & Ettema, R. (1977). Effect of sediment gradation on clear water scour. *Journal of the Hydraulics Division*, 103(10), 1209-1213.

Raudkivi, A.J. (1986). Functional trends of scour at bridge piers. *Journal of Hydraulic Engineering*, 112(1), pp. 1-13.

Richardson, J.R. and Richardson, E.V. (1994). Practical method for scour prediction at bridge piers.Proceedings, ASCE National Conference on Hydraulic Engineering, Buffalo, N.Y. 1–5.

Raudkivi,A.J.andEttema,R.(1983).Clearwaterscouratcylindricalpiers.*JournalofHy*

draulicEngineering,109(3),pp.338-350.

Shields, A. (1936). Application of similarity principles and turbulence researchto bed-load movement. Mitteilunger der Preussischen Versuchsanstaltfür Wasserbau und Schiffbau, Berlin, Germany, 26, pp. 5-24.

Shen, H.W., Schneider, V R. and Karaki, S. (1969). Local scour around bridge piers. *Journal of Hydraulic Division*, 95(6), HY6, 1919–1940.

Tseng, M. H., Yen, C. L., & Song, C. C. (2000). Computation of three-dimensional flow around square and circular piers. International journal for numerical methods in fluids, 34(3), 207-227.

Van Rijn, L. C. (1984). Sediment transport, part I: bed load transport. *Journal of Hydraulic Engineering*, 110(10), 1431-1456.

Yilmaz M., Yanmaz A. M. and M. Koken, (2017). Clear-water scour evolution at dual bridge piers. *Canadian Journal of Civil Engineering*,44(4), 298-307.